Critical behavior in the presence of a disordered environment

B. J. Frisken,* Fabio Ferri,† and David S. Cannell
Department of Physics, University of California, Santa Barbara, California 93106
(Received 16 January 1995)

We report details of experimental studies of the effect of dilute silica networks on critical phenomena for two binary fluid mixtures: lutidine-water (LW) and isobutyric acid-water (IBAW). For both mixtures, the primary effect of the silica is to induce a time-independent perturbation of the mixtures' concentration, making it spatially nonuniform. We interpret this as the static response of the critical system to the spatial nonuniformities of the silica concentration. We have measured this response by light scattering and find it is both temperature and concentration dependent, becoming strongly so in the vicinity of the consolute points of the mixtures. We observed no critical fluctuations for the LW-gel system. For the IBAW-gel system, time-dependent scattering was observed, and the temporal autocorrelation function of the scattered intensity revealed three regimes. Well away from the consolute point, the decay was exponential. By taking the effect of the time-independent response of the mixture to the silica gel into account, we found that the decay rates were comparable to those of the pure system. Correlation functions measured closer to the consolute point contained a significant nonexponential component for sufficiently large values of the scattering wave vector. This component is well fitted by either a stretched exponential or an activated form. From the amplitude of the normalized autocorrelation function we deduce that the critical fluctuations are suppressed in amplitude relative to those of the pure system as the consolute point is approached. Sufficiently near the phase boundary of the pure system, a very slowly decaying mode was also observed in the autocorrelation function. This mode died away hours after the small temperature change that induced it. A further temperature change toward the two-phase region induced it again, while a change in the opposite direction did not. We interpret this behavior as resulting from a phase separation process. IBAW-gel samples held deep in the two-phase region of the pure system for months ordered macroscopically, proving that this system has long-range order in the presence of such silica networks.

PACS number(s): 64.70.Ja, 64.60.Ht, 61.43.Hv

I. INTRODUCTION

In recent years, there have been both experimental and theoretical attempts to understand phase separation in fluid systems confined in porous or disordered media. Effort has focused on understanding the behavior in the regime where the fluid systems are single phased and on the phase-separation process itself. Both are dramatically affected by the presence of a disordering medium. The one-phase region of most systems appears to be characterized by strong, static, scattering and nonexponential temporal behavior near the critical points of the pure systems; the one-phase region will be the main subject of consideration in this paper. The phase separation process is also altered; macroscopic phase separation occurs on a much slower time scale than observed in the pure system. Experimental and theoretical results for phase separation of fluids and fluid mixtures in porous glasses are discussed, for example, in Ref. [1].

Work in this field is partly motivated by the goal of understanding the effects of random fields and/or exchange interactions on phase transitions of pure systems [2]. Disordered magnets were the first system of this type to be investigated following predictions by Imry and Ma [3] of macroscopic ordering in magnetic systems in the presence of a site-random field and the discovery by Fishman and Aharony [4] that this system could be realized by applying a uniform external magnetic field to doped antiferromagnetic samples. In zero field, this system is a realization of the random-exchange Ising model, and crosses over to random-field behavior as the external field is increased. Above a well defined temperature T_{eq}, the behavior is independent of sample history. Cooling the sample through this point in the presence of an external field leads to a frozen-domain state, while cooling in the absence of a field leads to long-range order below a second temperature T_c [5,6]. To date, most theoretical work has incorporated the assumptions that the magnitude of the random field is small, that it is uniformly distributed around zero, and that it is spatially uncorrelated. The random field presents energy barriers of height ξ^{ψ} to the movement of correlated regions, which implies that relaxation of the system will be activated, with characteristic equilibration times τ varying exponentially with the barrier height associated with the size ξ of the correlated region, $\tau(\xi) \sim \exp(\xi^{\psi}/k_B T)$.

*Present address: Department of Physics, Simon Fraser University, Burnaby, British Columbia, Canada V5A 1S6.
†Present address: Department of Physics, University of Milan at Como, Como, Italy.

Inspired by the work on magnetic systems and by early experimental work on fluids in agarose gels, Brochard and de Gennes suggested that the random-field Ising model might apply to vapor-liquid systems or fluid mixtures confined to porous media or in contact with a gel network [7,8]. Like some magnetic systems, fluid systems are members of the spin-1/2 Ising universality class, with the important difference that the order parameter (density or concentration) is conserved in this case, while for magnetic transitions it is not. Further work indicated that metastability and activated dynamics were also to be expected for the conserved order-parameter case [9]. In these systems, surface forces at the interface between the fluid and the solid medium result in preferential attraction of fluid by the solid medium leading to density or concentration perturbations. Thus, solid media can presumably be modeled as exerting a spatially varying field on the fluid system. These ideas have led to controversy in the interpretation of experimental results for fluid systems in the presence of disorder and it is not clear that all such systems will fit into a random-field picture. Experimental realizations of fluid systems have incorporated the use of both porous glasses, where the fluid is confined to a pore space, and various gels, where the fluid surrounds a dilute gel network. In both cases, though, the structure is spatially correlated, resulting in correlated rather than spatially random fields. The medium actually applies a field of nonzero mean, although this can be cancelled by adjusting the concentration or density of the fluid. Furthermore, to reach the regime considered by random-field models, the correlation length of the system should be larger than the length scale of the disorder; this condition has not been observed in fluid systems and appears to be preempted by a phase-separation process [10]. Some experimental studies of binary fluids confined to porous glasses [11–13] have been successfully discussed in terms of wetting in a single pore model [14], but more extensive work is clearly needed to understand these systems.

Experiments involving flexible or noncovalently crosslinked gels such as agarose, polyacrylamide, and gellan gum gels revealed strong light scattering and cloud points near the pure system's coexistence curve [15,16]. These researchers observed that the region of enhanced scattering was broader in temperature than seen in the pure system, and they interpreted this as a broadening of the transition. Most samples revealed small-amplitude temporal fluctuations in the scattered intensity. More extensive measurements of a mixture of isobutyric acid and water in gellan gum gels [17] revealed critical fluctuations having both a diffusive component (i.e., with a decay rate $\Gamma \propto q^2$, where q is the wave vector of the fluctuation) and a second exponential, but nondiffusive, component. The amplitude of the nondiffusive term increased as the temperature T approached the critical temperature of the pure system T_c. The interpretation of these experiments has remained problematic because such gels are either flexible or not covalently cross-linked and might participate in the phase-separation process (the gels can swell or shrink as conditions change), and because the structure of these gels has not been well characterized.

Studies of lutidine-water (LW) mixtures in Vycor, a porous glass with pore diameters of ~ 70 Å and a porosity of $\sim 30\%$, have involved both light scattering [11] and small angle neutron scattering [12,13]. The measurements were done in the absence of a supernatant fluid, ensuring that the samples were kept at constant composition. In contrast to the results discussed above, the intensity scattered by the samples did not change appreciably until well into what would be the two-phase region of the pure system. Studies of the temporal behavior of the scattering revealed activated dynamics and metastability, but again only well into what would be the two-phase region for the pure system. Also, samples were characterized by the lack of a well defined phase-separation point. Recently, these results have been discussed in terms of wetting and domain growth [14].

Studies of phase-separation of ^{4}He and N_2 in aerogels (silica networks formed by hypercritically drying gels created by polymerization of a molecular precursor) revealed a drastically narrowed coexistence curve located under the pure system's coexistence curve and characterized by an exponent similar to that for the coexistence curve of pure fluids [18,19]. Dynamic light scattering measurements on N_2 samples revealed activated behavior consistent with random-field effects but no crossover to behavior characteristic of the pure system far from the critical region. Most of these measurements were made in a regime where the sample was scattering quite strongly, which makes interpretation difficult. These experiments have been discussed in terms of an asymmetrically distributed random-field model that exhibits behavior differing significantly from that of the traditional random-field Ising model [20].

Recent studies have been made of a mixture of carbon disulfide and nitromethane at what would be the critical concentration of the pure system [21] in a porous glass similar to Vycor but with larger pore sizes. Again, this system showed strong static scattering and only weak temporal fluctuations. In the presence of an external reservoir, the dynamics were characterized by a double exponential, while an isolated system showed nonexponential behavior.

In summary, although the critical behavior of these and other diverse systems is well understood in their pure states, the response of critical systems to the surface fields and/or boundary conditions associated with pores or the strands of a gel network is complex and has not been satisfactorily explained. In general, confined fluids and fluid mixtures fail to exhibit the long-range spatially correlated fluctuations and the concomitant extreme slowing down of temporal fluctuations associated with the critical points of the pure systems. Temporal fluctuations are weak, if they are present at all. Instead, the main response seems to be strong, time-independent scattering, which grows in amplitude as the critical region is approached.

As we will show below, this time-independent scattering is due to time-independent concentration fluctuations in the fluid mixture that are induced by the gel or porous medium. In fact, it is well known that surfaces inevitably attract one of two species preferentially,

or prefer either the liquid or vapor phase when in contact with a single fluid [22]. For example, in a critical system near a planar substrate, the composition of the mixture will be perturbed over a distance from the substrate comparable to the bulk correlation length, and the amount of adsorbed material will diverge as the critical point is approached [23]. This phenomenon is known as critical adsorption. If the surfaces of the gel or porous medium are modeled in terms of a surface field that acts on molecules or atoms near the surface, then such a field would be expected to induce a strongly temperature- and concentration-dependent, possibly nonlinear, response in a critical system, provided the surface field couples to the critical system's order-parameter (concentration for a mixture, or density for a single fluid) [8]. If the response is linear, it should diverge near the critical point because the order-parameter susceptibility diverges strongly at the critical point. Presumably, the actual response will be limited by nonlinearities.

In order to address these issues, we have used light scattering to study the effect of dilute silica gels on critical phenomena in two binary mixtures. Silica gels are good candidates for these studies; they are rigid, do not appear to swell or shrink significantly, and can be made to have different "mesh sizes." They are rigid and static in the sense that light scattered from a silica gel containing only pure water exhibits no observable temporal fluctuations in its intensity as measured by dynamic light scattering. Also, their structure can be very accurately characterized using scattering techniques. The gels used in these studies were formed by polymerization of a molecular precursor in water and were never dried. Light-scattering studies [24] revealed that the gels scatter like fractal objects, with a fractal dimension $D_f \sim 2.2$ at length scales smaller than a crossover length ξ_x, and like a random collection of fractal objects for length scales $\geq \xi_x$. The length scale ξ_x could be varied from $\lesssim 100$ Å to $\gtrsim 2$ μm by changing silica concentration and to some extent gelation conditions. This scattering behavior results from fluctuations in local silica concentration that are spatially correlated up to the length scale ξ_x and rapidly become uncorrelated for distances $\gtrsim \xi_x$.

Our first studies involved various mixtures of 2,6-lutidine and water (LW) in silica gels with crossover lengths of 250, 1200, and 1600 Å [25]. These studies failed to detect any critical dynamics. However, they showed that the distribution of the intensity of scattered light with scattering wave vector q resembled in form that of the gel in pure water, with an amplitude that appeared to diverge as the phase-separation temperature was approached. These results were interpreted in terms of preferential attraction of lutidine by the silica gel, leading to lutidine-rich fluid near the gel strands. Because the refractive index of lutidine is similar to that of silica, deviations in local silica concentration from the sample average were effectively enhanced by the excess lutidine to the point where scattering from them masked any critical scattering by the remaining mixture.

Hoping to avoid the very strong time-independent scattering that dominated the behavior of the LW-gel system, we sought a second fluid mixture for study. The system chosen was isobutyric acid and water (IBAW) [10]. In this case, water was preferentially attracted to the silica, which led to a decrease in the scattered intensity as compared to that of the gel in pure water. Since water has the lowest refractive index of the three components, as it is attracted by the silica it reduces the local refractive index of the silica-rich regions, bringing them closer in refractive index to that of the sample as a whole, leading to decreased scattering. This decreased scattering had two consequences: it meant that the critical region could be approached without encountering serious multiple scattering, and it allowed observation of critical fluctuations by dynamic light scattering. We observed three dynamic regimes. In the one-phase region, well above the two-phase boundary of the pure system, we observed exponential relaxation of fluctuations, which is characteristic of the pure system. Closer to the two-phase boundary of the pure system, the dynamics included a nonexponential component, first observable at small length scales (large q) and then at longer and longer length scales as the critical point was approached. We were able to fit this component with either a stretched exponential or an activated form. Near the pure system's coexistence curve, the dynamics abruptly developed a slow mode (decay time $\sim$10 s) which died away in amplitude over a period of hours. This behavior was observed following small changes in temperature toward the two-phase region, but never upon stepping temperature back toward the one-phase region. After the slow mode died away, the system required many hours to return to equilibrium when returned to the one-phase region. We associate this third dynamic regime with phase separation of the mixture inside the gel.

II. EXPERIMENT

A. Sample preparation

The silica gels were grown from solutions of $Si(OCH_3)_4$ (tetramethylorthosilicate, or TMOS) in water using a two-step process [26]. The TMOS was first hydrolyzed by dissolving it in dilute HCl (pH 2.0) and stirring the solution for about one hour. An approximately equal volume of dilute NaOH (of appropriate pH) was then added to increase the pH of the final solution into the range $5.0 < \text{pH} < 6.4$; this step initiated a condensation reaction. The solutions were then filtered through 0.22 μm filters (Millipore MF-type) into glass scattering cells. Samples which were to be used with mixtures of lutidine-water or isobutyric acid–water were gelled in cells of inner diameters 4.72 mm and 9.91 mm, respectively. The solutions gelled at room temperature. After the gels were aged for a time roughly equal to ten times the gelation time, as judged by a sharp decrease in the fluidity of the samples, they were exposed to mixtures of either lutidine-water or isobutyric acid–water at various concentrations spanning the critical concentration. This was carried out at temperatures in the one-phase region well away from the critical temperature of the respective mixture so that the mixtures were homogeneous. The

supernatant mixture, which had a volume twice that of the gel, was mixed daily to eliminate concentration gradients and replaced once a week for four weeks. Thus, before they were studied the gels had been exposed to four different supernatant mixtures of the same initial concentration. During the equilibration process, the LW samples were sealed with viton stoppers and the IBAW samples were sealed with teflon stoppers. Viton did not seem to affect the phase separation temperature of pure LW mixtures, but had a pronounced effect on that of IBAW mixtures. After equilibration, the supernatant mixture above the gels was poured off so that the average concentration of the mixture inside the gel could not change during the measurements. The LW samples were left with their viton stoppers, while the IBAW samples were flame sealed without freezing the samples.

B. Apparatus

The light-scattering apparatus [27] used in these experiments collects light scattered at fixed angles ranging from 2.7° to 163°. Each angle θ corresponds to a scattering wave vector $q = (4\pi n/\lambda)\sin(\theta/2)$, where $\lambda = 6328$ Å and n is the refractive index of the sample. Measurements of toluene were made to calibrate the scattering measured by the instrument in absolute units. Samples were held in a water bath temperature controlled to ± 0.3 mK. The total (time-averaged) intensity scattered by the samples was measured as a function of scattering wave vector q. The total intensity scattered is proportional to the Fourier transform of the spatial correlation function of the dielectric constant fluctuations and yields information about the structure of the sample. Fluctuations of the scattered intensity were analyzed by a correlator (ALV5000) that computed the temporal intensity-intensity autocorrelation function. These dynamic light-scattering measurements allow determination of decay rates and diffusion coefficients.

Each scattering channel associated with the fixed angles of the apparatus images a small slit $\simeq 0.1$ mm wide into the sample center with a magnification of 0.65, and accepts only scattered light that originates from within that image. The incident beam is focused to a diameter of ~ 0.1 mm coincident with the images of the slits at the sample center. This arrangement results in speckle with effective dimensions of order 1 mm at the lenses used to image the slits, which are located a distance of 170 mm from the sample center. A circular aperture is positioned very near each lens and serves to define the acceptance solid angle of each channel. For total intensity measurements, the apertures accepted light from about five speckles, but for the dynamic measurements the sizes of the apertures were reduced so as to accept only a fraction of a single speckle. This increased the amplitude of the mean-squared intensity fluctuations $\langle I^2\rangle$ relative to the square of the mean intensity $\langle I\rangle^2$. The former determines the amplitude of a measured autocorrelation function at zero delay time, while the latter sets the baseline to which it decays at large delay times.

C. Sample characterization

The silica-gel structure was characterized by measurements of the total scattered intensity [24]. Figure 1 shows data and fits for gels made at pH 5.7 ± 0.1 spanning the entire concentration range studied in Ref. [24]. The q-dependent intensity of the scattered light, which is directly proportional to the scattering cross section per unit volume (or Rayleigh factor) $S(q)$, is well described by the equation [28]

$$S(q) = \frac{S(0)}{[1+q^2\xi_x^{\,2}]^{(D-1)/2}} \frac{\sin[(D-1)\tan^{-1}(q\xi_x)]}{(D-1)q\xi_x} \quad , \tag{1}$$

where ξ_x is a crossover length and D is the fractal dimension.

This Rayleigh factor reflects the fact that the gel scatters uniformly on long length scales ($q < \xi_x^{-1}$) and like a mass fractal at small length scales ($q > \xi_x^{-1}$). Fit results for D ranged from 2.1 for the lightest gels studied up to ~ 2.3 for the most concentrated gels whose fractal dimensions we were able to estimate by light scattering. Subsequent neutron-scattering studies [29] on similar gels grown in D_2O have shown that this structure persists to q values as large as 0.1 Å^{-1}. However, the neutron-scattering studies reveal no dependence of D on the gel concentration. For all of the gels studied by light scattering, we found a simple relation between $S(0)$, D, ϕ, and ξ_x,

$$S(0) = B\,\Gamma(D)\,\phi^2\xi_x^3 \quad , \tag{2}$$

with $B = (1.4 \pm 0.1) \times 10^{18}$ cm^{-4}, and where $\Gamma(D)$ is the gamma function.

In general, $S(q)$ is proportional to the Fourier trans-

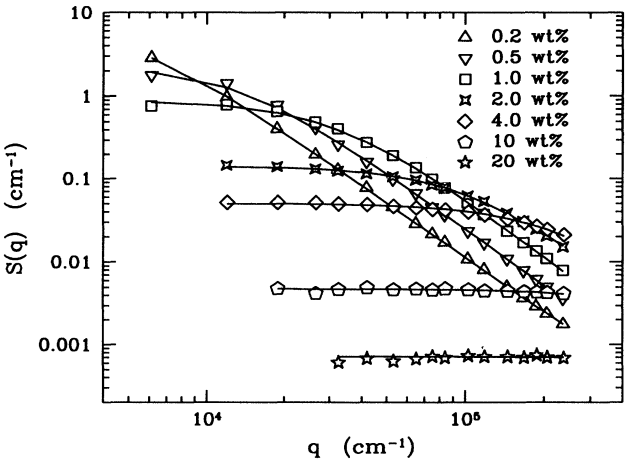

FIG. 1. Rayleigh factor as a function of scattering wave vector for hydrogels of different silica weight fractions made in the pH range 5.7 ± 0.1. The solid curves are the results of fitting Eq. (1) to the data. As may be seen, denser gels scatter less light and have smaller crossover lengths.

form of the density-density correlation function of the scattering medium. The gels studied here are then consistent with a correlation function

$$g(r) \equiv \langle \delta\phi(\vec{r})\delta\phi(0)\rangle \tag{3}$$

given by

$$g(r) = 1.8\,\bar{\phi}^2 e^{-r/\xi_x}/(r/\xi_x)^{3-D} \quad , \tag{4}$$

where $\delta\phi(\vec{r})$ is the local deviation from the average volume fraction of silica $\bar{\phi}$. Thus, the structure of the gels is consistent with deviations in local silica concentration, which are correlated up to distances of order ξ_x, with these correlations falling off rapidly for length scales $\gtrsim \xi_x$. Note that because the scattering measurements for the gels were made in absolute units, we obtained a quantitative result for the correlation function $g(r)$, including its actual numerical amplitude. Rather remarkably, all the hydrogels studied had correlation functions given by Eq. (4). The individual gels differed only in $\bar{\phi}$, ξ_x, and perhaps D.

Light-scattering measurements were also made to characterize the critical properties of both of the pure-mixture systems. It is useful to note here that the LW system has an inverted coexistence curve, while the IBAW system has a regular one with the two-phase region lying below the one-phase region in temperature. Measurements of the angular distribution and the total scattered intensity determined the susceptibility and correlation length of the order-parameter fluctuations as a function of temperature and concentration. Dynamic light scattering was used to determine the associated decay rates and diffusion coefficients. A near-critical LW mixture of 29.1 wt.% lutidine yielded a critical temperature of 33.40 °C and a correlation length amplitude of 2.1 Å. IBAW mixtures at 29.0, 34.1, 38.8, 44.0, and 49.0 wt.% IBA were studied in order to quantify the effect of concentration on the critical properties. Measurements of the near-critical sample (38.8 wt.%) yielded a critical temperature of 26.67 °C and a correlation length amplitude of 3.61 Å. Figure 2 shows the temperature and concentration dependence of $S(0)$, which is the small q limit of the scattered intensity and is proportional to the order-parameter susceptibility. Figure 3 shows the temperature and concentration dependence of the diffusion coefficient for the pure IBAW samples. The diffusion coefficient was obtained by fitting the intensity-intensity autocorrelation functions to a single exponential. The q-dependent decay rates were accurately proportional to q^2, and the proportionality factor was twice the diffusion coefficient.

To determine the concentration of the mixtures inside the gel-mixture samples, the concentrations of the fluid components were measured by gas-phase chromatography after all the light scattering studies had been completed. These measurements were carried out on an HP5880 gas chromatograph. The LW samples were analyzed on a blood alcohol column (60/80 Carbopack B/5% Carbowax 20M), and the IBAW samples were analyzed on an acid washed column (80/120 Carbopack B/6.6% Carbowax 20M), both obtained from Supelco. To make these measurements, the samples were crushed and diluted in 1-pentanol to make a 1 vol.% sample-solvent mixture. The 1-pentanol had been dried over molecular sieves and independently measured to calibrate for water and methanol content. Measurements of gels containing only water mixed with a known amount of either isobutyric acid or lutidine showed that neither component of the mixture adhered to the silica after dilution by 1-pentanol. The samples were measured and compared to known mixtures, also diluted to make 1 vol.% sample-solvent mixtures. In this way, it was possible to measure the weight fraction of both the isobutyric acid or lutidine component and the methanol component of the fluid portion of the sample. The methanol is a by-product of the gelation process and is an impurity that can cause shifts of the critical temperature (1 vol.% methanol will depress

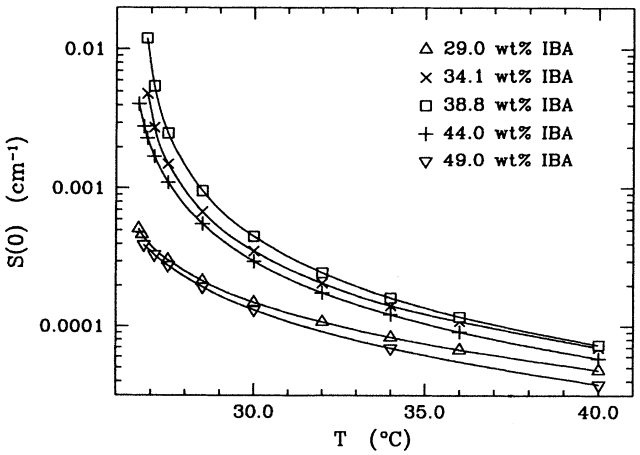

FIG. 2. Temperature dependence of $S(0)$, which is proportional to the order-parameter susceptibility, for pure IBAW samples of various concentrations spanning the critical concentration. The lines are guides for the eye.

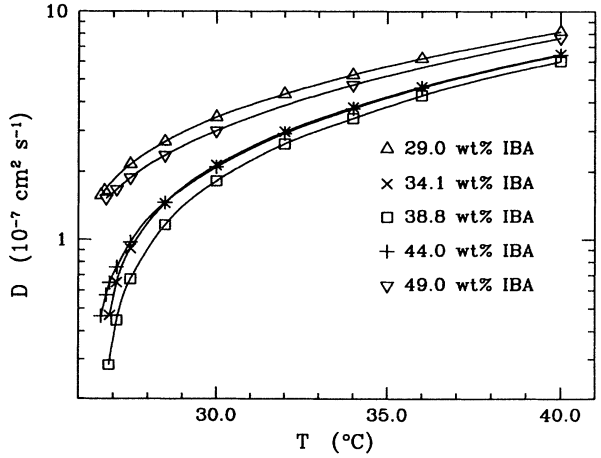

FIG. 3. Temperature dependence of the diffusion coefficient of pure IBAW samples of various concentrations spanning the critical concentration. The lines are guides for the eye.

T_c by ~ 4 °C for the IBAW system and will increase T_c by ~ 2 °C for the LW system). It was determined that the concentration of methanol in the IBAW-gel samples was less than 0.01 vol.% and in LW-gel samples was less than 0.1 vol.%. NaCl is also a by-product of the gelation process (a 0.01M NaCl concentration will increase T_c by ~ 2 °C for the IBAW system and decrease T_c by ~ 1 °C for the LW system). Its concentration in the gel-mixture samples was not measured, but, unless it failed to partition equally between the supernatant and the gel, its final concentration should have been less than $\leq 2.0 \times 10^{-5}$ M for any sample studied.

D. Sample measurement

Studies of the gel-mixture samples involved both total intensity and dynamic light-scattering measurements. During total intensity measurements, the samples were rotated about their axes at 5 Hz to average over many sample orientations. This is not necessary for most systems studied by light scattering because samples normally undergo thermal fluctuations, and time averaging alone is sufficient to obtain a representative average. Since the gel structure is static, gel samples are not ergodic, and rotating the sample or some other such device is necessary to ensure that a representative average of the sample structure is measured [30]. Since the temporal autocorrelation function of the scattered light, measured while the sample was rotating, had a correlation time of 0.02 ms, we estimate that about 10^4 independent samples were measured by rotating the sample. During dynamic measurements, the samples were clamped in place to prevent any motion that might cause spurious time dependence of the scattered intensity.

Measurements were performed as a function of temperature, almost entirely in what would be the one-phase region of the pure mixtures. Typically, the experiments started far from the critical region and gradually approached it. The samples were left an hour between temperature changes to allow for equilibration. Some backtracking along the temperature path was made to check that slow changes in the scattered intensity were not occurring and to ensure that equilibrium had been reached. To check that the samples had not been irreversibly altered during the experiments, and to ensure that the initial conditions could be reproduced, the temperature was changed back to the starting temperature after closest approach to the critical region had been made. For all the samples we studied, the static scattering results were reproduced to within ±10%.

III. RESULTS AND DATA ANALYSIS

A. Statics

1. *Measurements of the total scattered intensity*

Response of the fluid mixtures to the silica gels was noticeable even well away from the critical region. The concentrations of the fluid mixtures in the gels were different from those of the baths with which the samples were equilibrated; in the case of LW gels, the concentration in the gels was higher in lutidine, and in the case of IBAW gels, the concentration in the gels was higher in water. These observations show that lutidine was preferentially attracted by the silica from the LW mixtures, while water was preferentially attracted from the IBAW mixtures. This is consistent with a quantitative analysis of how the scattered intensity changed with temperature, as described below.

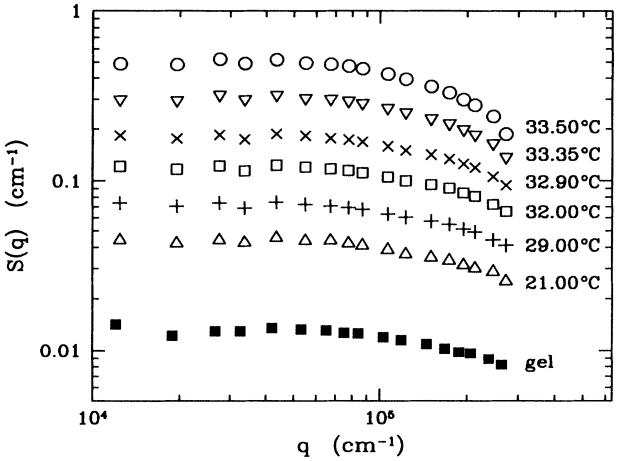

FIG. 4. Rayleigh factor as a function of scattering wave vector for various temperatures for a sample with 4 wt.% silica and which contained 37 wt.% lutidine. The gel had a crossover length of 300 Å. The sample always scattered more than a similar gel containing only water (solid squares). As the temperature increased, the absolute scattering increased with only a slight change in q dependence.

Total scattered intensity measurements were made for LW gel samples containing mixtures of various concentrations in gels containing 1.00, 2.00, and 4.00% silica by weight, which corresponds to 0.46, 0.92, and 1.86% silica by volume, respectively. These gels had crossover lengths of 1600, 1200, and 250 Å, respectively.

Although we focused on samples containing 4 wt.% silica and 21, 26, 31, 34, 37, and 41 wt.% lutidine, similar behavior was observed for all samples. The dependence of the scattering cross section $S(q)$ upon the scattering wave vector q was nearly identical to that of the gel-water system for all temperatures and gel-mixture concentrations, while the overall scattered intensity increased strongly as the temperature was increased towards the two-phase boundary of the pure system. Figure 4 shows $S(q)$ as a function of q at various temperatures for a sample which contained 4 wt.% silica and 37 wt.% lutidine. At the temperatures shown in Fig. 4, there was no indication of hysteresis, and we believe that all of the samples were still in the one-phase region for the gel-mixture system.

These samples scattered quite strongly, and double scattering corrections [31] have been made. To minimize double scattering, we focused on samples containing 4 wt.% silica, since samples containing higher silica

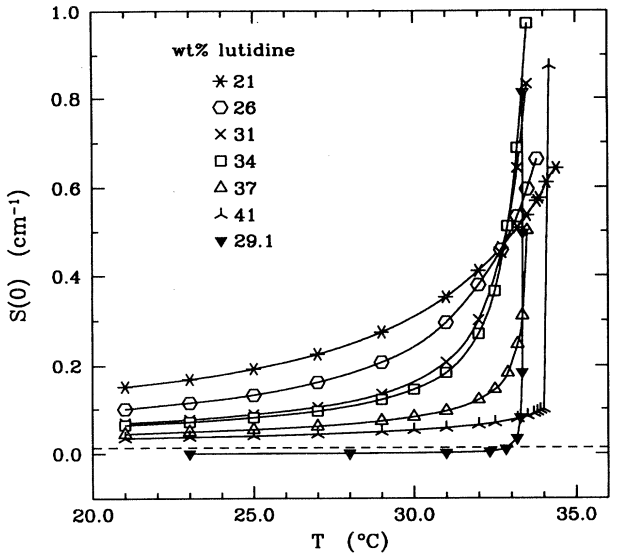

FIG. 5. Summary of the temperature dependence of $S(0)$ for 4 wt.% silica gels with various lutidine concentrations. The gels have crossover lengths of about 300 Å. As the temperature was increased and the phase boundary of the pure system was approached, the intensity increased for all samples. The dashed line shows the scattering from a similar gel containing only water; data for a pure lutidine-water mixture near the critical concentration at 29.1 wt.% is shown by solid inverted triangles. The solid curves through the data are included only as guides for the eye.

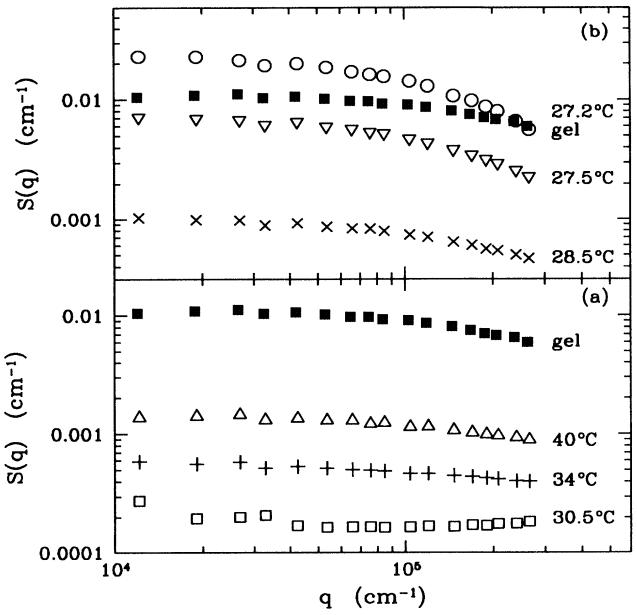

FIG. 6. Rayleigh factor as a function of scattering wave vector at various temperatures for a 4 wt.% silica gel containing 27 wt.% IBA. The gel had a crossover length of 300 Å. (a) Far away from the two-phase boundary of the pure system (40 °C), the structure was similar to that of the gel in pure water (solid squares) but had a decreased intensity due to preferential attraction of water. The intensity decreased as the two-phase boundary of the pure system was approached and more water was adsorbed, reaching a minimum at 30.5 °C. (b) Closer to the two-phase boundary of the pure system, the absolute intensity increased as the two-phase boundary of the pure system was approached and the structure deviated from that of the gel in pure water (solid squares).

concentrations scatter less light. None of the data from these samples required corrections of more than 10%. Although $S(q)$ was generally quite similar to that of the gel-water system, slight changes ($< 10\%$) in $S(q)$ were observed in the samples that we believe approached closest to the critical point, but because of the strong scattering, interpretation of these changes is probably not justified.

Figure 5 summarizes the temperature dependence of $S(0)$, the large length scale limit of $S(q)$, for six samples and compares it to $S(0)$ measured for a pure mixture of 29.1 wt.% lutidine, which is near the critical concentration, as shown by solid inverted triangles. The dashed curve shows the scattering by a gel from the same batch that contained only water. For all of these samples, $S(0)$ increased monotonically with increasing temperature. The scattering from samples containing less lutidine increased less rapidly than it did for those at higher concentration. For all samples, the intensity increased much less precipitously than it did for the pure mixture. This effect is similar to that described in Ref. [15], where it was interpreted as a broadening of the transition. As will be discussed below, this effect can be explained in terms of preferential attraction of one component of the mixture by the silica, and the light-scattering data can be used to quantitatively determine the response of the fluid mixture to the field imposed by the gel.

Studies of the total scattering intensity from IBAW-gel samples focused on samples containing 4 wt.% silica and 26, 27, and 28 wt.% IBA. The gels had crossover lengths of about 300 Å. The scattering behavior was different from that of the LW gel samples, but was the same for all IBAW-gel samples. Far from the two-phase boundary of the pure system, the q dependence of the scattering was similar to that of a gel from the same batch containing only water, but the intensity scattered was less. The reduced scattering intensity had the advantage that all of the measurements could be made in the single scattering regime, with no correction for double scattering necessary. As the temperature was decreased towards the two-phase boundary of the pure system, the intensity decreased, reaching a minimum at a concentration-dependent temperature T_{min}. As the temperature was decreased further towards the two-phase boundary of the pure system, the scattering intensity increased, and the structure began to deviate from that of the gel-water sample. Figure 6 shows $S(q)$ as a function of q at various temperatures for a sample with 4 wt.% silica and 27 wt.% IBA. The structure of a gel made in the same batch and containing only water is shown by the solid squares. Figure 7 summarizes the temperature dependence of $S(0)$ for the three samples being considered here. The minimum is marked by an arrow for each sample; T_{min} increased

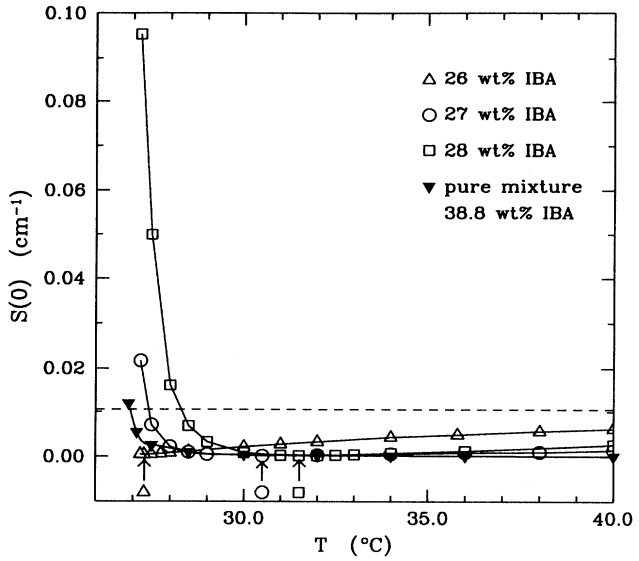

FIG. 7. Summary of the temperature dependence of $S(0)$ for 4 wt.% silica gels of various isobutyric acid concentrations. The gels had crossover lengths of about 300 Å. As the temperature was decreased and the two-phase boundary of the pure system was approached, the intensity first decreased, then reached a minimum, and finally increased. The minimum occurred at lower temperatures for gels of lower IBA concentration and is marked on the graph for each sample. Data for a pure isobutyric acid-water mixture near the critical concentration at 38.8 wt.% are shown by solid inverted triangles. The solid curves are included only to guide the eye. The dashed line shows the scattering from a similar gel containing only water.

with increasing IBA concentration. The dashed line represents the scattering from the gel-water sample.

2. *Analysis*

These results can be used to quantify the mixture's response to the silica gel, which presumably occurs because of the surface field associated with the gel strands. In practice, the gel exerts both an average field $\bar{h}$ and a spatially varying field $\delta h(\vec{r})$ and we assume that the deviations $\delta h(\vec{r})$ of the field are proportional to the deviations in local silica volume fraction,

$$\delta h(\vec{r}) \propto \delta\phi_s(\vec{r}) \quad . \tag{5}$$

This assumption is strongly supported by the fact that the scattering from the gel-mixture systems has essentially the same q dependence as that of the gels in pure water. The concentration difference between the fluid in a gel and that of a bath with which it is in equilibrium may be viewed as the mixture's response to the spatial average or mean field associated with the gel. The nonuniformity of the local silica concentration results in local deviations of the mixture's concentration from the average. Since it is long-wavelength inhomogenieties that are responsible for the scattering of light, we may interpret light-scattering data for the gel-mixture samples quantitatively to determine the response of the mixture to this spatially varying field. Since the shortest wavelength fluctuation probed was ≈ 2400 Å, this represents a coarse-grained response.

For mixtures confined within rigid gels, the amplitude of the scattered electric field corresponding to any particular scattering wave vector consists, in general, of a time-independent portion and time-dependent fluctuations. In the case of the LW-gel samples, where the magnitude of the scattering was generally large in comparison to what was observed for the pure system at similar temperatures and concentrations, no time-dependent portion was observed. The sensitivity of these measurements was such that fluctuations at 15% of the level displayed by pure mixtures within 0.5 °C of the critical temperature should have been detected. Since no time-dependent contribution to the scattering was observed, it was clear that the fluid mixture had responded to the gel by establishing time-independent concentration fluctuations, which enhanced the dielectric constant fluctuations due to the gel itself. In the case of the IBAW-gel samples, both static and time-dependent contributions were clearly present. The contribution of the fluctuating component to the total scattered intensity was deduced from the total intensity and the amplitude to baseline ratio of the intensity-intensity autocorrelation function, as described below. Even for the IBAW-gel samples, the scattering was predominantly static, except near the scattering minimum, where the time-dependent portion was significant.

We may interpret the scattering for the gel-mixture systems quantitatively as follows. The scattering cross section at a particular angle is proportional to the mean-squared amplitude of the corresponding spatial Fourier component of the dielectric constant, $S(q,t) \propto \langle \mid \delta\epsilon(q,t) \mid^2 \rangle$, where the angular brackets denote an ensemble average, which we approximate experimentally by rotating the samples continuously while measuring the total scattered intensity. The dielectric constant depends on the local concentrations of silica and the two fluid species. Neglecting any volume change upon mixing, the Clausius-Mossotti relation for multicomponent systems can be used to calculate $\epsilon(\vec{r},t)$,

$$\frac{\epsilon(\vec{r},t)-1}{\epsilon(\vec{r},t)+2} = K_s\phi_s(\vec{r}) + K_a\phi_a(\vec{r},t) + K_n\phi_n(\vec{r},t) \quad , \tag{6}$$

where $K \equiv (\epsilon-1)/(\epsilon+2)$, and $\phi(\vec{r},t)$ is the local volume fraction of the different chemical species in the sample as indicated by the subscripts s, a, and n, which refer to silica, the preferentially attracted, and nonpreferentially attracted species, respectively. In the case of LW gels, lutidine is the attracted species, while in IBAW gels, it is water. The local silica concentration is time independent, but the local concentrations of the two fluids will generally have both static and time-dependent deviations from their average values. From the differential of Eq. (6), noting that $\epsilon(\vec{r},t)+2 \simeq \bar{\epsilon}+2$, that $\phi_s+\phi_a+\phi_n = 1$, and Fourier transforming, the dielectric constant fluctuations can be written as

$$\delta\epsilon(\vec{q},t) = \frac{(\bar{\epsilon}+2)^2}{3}[(K_s - K_n)\delta\phi_s(\vec{q}) + (K_a - K_n)\delta\phi_a(\vec{q},t)] \quad , \tag{7}$$

where $\delta\phi$ is the local deviation from the average, and a bar denotes the sample average. The quantity $\delta\phi_a(\vec{q},t)$ can be decomposed into a static portion $\delta\phi_a^{stat}(\vec{q})$, and a zero-mean fluctuating portion $\delta\phi_a^{fluct}(\vec{q},t)$,

$$\delta\phi_a(\vec{q},t) = \delta\phi_a^{stat}(\vec{q}) + \delta\phi_a^{fluct}(\vec{q},t) \quad . \tag{8}$$

Although the second term has zero mean, it contributes to the total scattered intensity through its mean-squared value. Because of our experimental observations, we associate the first term with the static response of the mixture to the silica gel, and the second term with the critical fluctuations of the fluid.

Concentrating on the static term, which is dominant in most of the measurements, we model the static deviation in the concentration of the preferentially-attracted species $\delta\phi_a^{stat}(\vec{q})$, as being proportional to the deviations in silica concentration, $\delta\phi_s(\vec{q})$. That is, excess silica in a particular region results in a time-average excess of the preferentially attracted species. This model can be expressed very simply as

$$\delta\phi_a^{stat}(\vec{q}) \equiv \alpha(\vec{q},T)\,\delta\phi_s(\vec{q}) \quad , \tag{9}$$

which defines the static response function $\alpha(\vec{q},T)$. This model is consistent with the theoretical work of de Gennes [8] and analysis of scattering from diluted antiferromagnets [6]. Using Eqs. (8) and (9), the static portion of the total scattered intensity for the gel-mixture system $S_{gm}^{stat}(q)$, can be obtained from the square of the time-independent portion of $\delta\epsilon(\vec{q},t)$. It can be expressed in terms of the total scattered intensity for the gel-water system $S_{gw}(q)$,

$$S_{gm}^{stat}(q) = \frac{(\bar{\epsilon}_{gm}+2)^4}{(\bar{\epsilon}_{gw}+2)^4}\left[\frac{(K_s - K_n) + \alpha(q,T)\,(K_a - K_n)}{K_s - K_w}\right]^2 S_{gw}(q) \quad . \tag{10}$$

Water, IBA, silica, and lutidine have refractive indices of approximately 1.33, 1.39, 1.46, and 1.49, corresponding to K values of 0.20, 0.24, 0.27, and 0.29, respectively. The scattering results are consistent with lutidine being preferentially attracted in LW gels and water being attracted in IBAW gels; as α increases upon approaching the critical region, the factor multiplying $S_{gw}(q)$ in Eq. (10) increases monotonically for LW gels and first decreases before increasing for IBAW gels, in agreement with the data. These observations are consistent with gas chromatographic analysis of gels that have been well equilibrated with supernatant mixtures.

Knowing which species is attracted, the data can be analyzed using Eq. (10), and the function $\alpha(q,T)$ can be deduced. In the case of LW gels, the static response was the sole measurable contribution to the total scattered intensity. In the case of IBAW gels, this contribution was found by subtracting the fluctuating contribution from the total scattered intensity, where the fluctuating contribution was first extracted from data for the intensity-intensity autocorrelation function, as described below in the section on dynamic measurements.

One additional subtlety that should be noted is that $\alpha = 0$ does not correspond to the case of no response. In the absence of preferential attraction, the volume fraction of both fluid species is reduced by the presence of excess silica simply because the fluids are excluded from the volume occupied by the silica. Thus, in the case of no response, the local volume fraction of the attracted species fluctuates by an amount given by

$$\delta\phi_a(\vec{q}) = -\bar{\phi}_a^{mixt}\,\delta\phi_s(\vec{q}). \tag{11}$$

Here $\bar{\phi}_a^{mixt}$ is the average volume fraction of the attracted species in the fluid portion of the sample (as opposed to the entire volume), and is given by

$$\bar{\phi}_a^{mixt} = \frac{\bar{\phi}_a}{\bar{\phi}_a + \bar{\phi}_n} = \frac{\bar{\phi}_a}{1 - \bar{\phi}_s} \quad . \tag{12}$$

Thus the quantity $\alpha(q,T) + \bar{\phi}_a^{mixt}$ is a more precise measure of the response caused by preferential attraction of one species by the silica than is $\alpha(q,T)$, itself.

We find that the $q \to 0$ limit of $\alpha(q,T)+\bar{\phi}_a^{mixt}$ increases strongly as the temperature approaches the two-phase

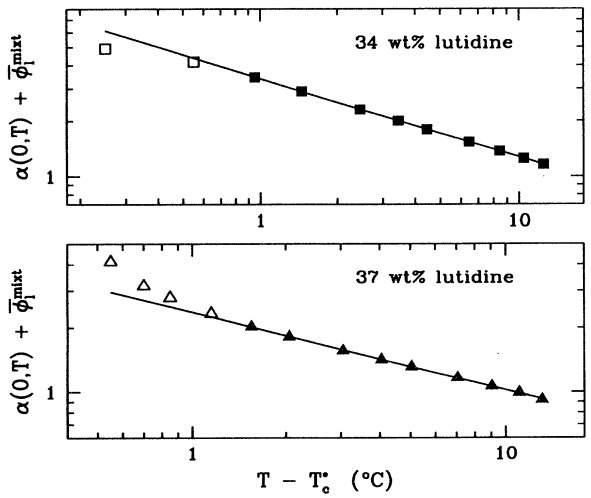

FIG. 8. Temperature dependence of $\alpha(q=0,T) + \bar{\phi}_l^{mixt}$ (see text) for two LW gel samples. The solid line is the result of fitting a power law with an adjustable critical temperature and susceptibility exponent to the data shown as solid symbols. Data shown as open symbols were excluded from the fit.

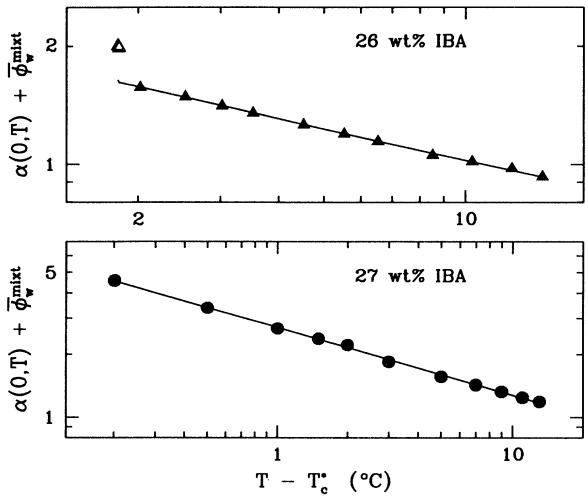

FIG. 9. Temperature dependence of $\alpha(q=0,T)+\bar{\phi}_w^{mixt}$ (see text) for two IBAW gel samples. The solid line is the result of fitting a power law with an adjustable critical temperature and susceptibility exponent to the data shown as solid symbols. Data shown as open symbols were excluded from the fit.

boundary of the pure system for samples that are not too far from the critical concentration. Away from the two-phase boundary of the pure system, this quantity can be fit to the form $\alpha(q=0,T)+\bar{\phi}_a^{mixt}=\alpha_0|T-T_c^*|^{-\gamma^*}$. The parameters T_c^* and γ^* are convenient fitting parameters and represent an effective critical temperature and susceptibility exponent, respectively. For smaller $|T-T_c^*|$, deviations from the power law fits are systematic; samples sufficiently rich in the attracted species have α increasing faster than a power law fit to the data far from T_c^*, and those sufficiently poor in that species have α increasing more slowly. Figures 8 and 9 show typical results for $\alpha(q=0,T)+\bar{\phi}_a^{mixt}$ for LW gels and IBAW gels, respectively. All of the mixtures were in 4.0 wt.% silica gels. Results of the fits are listed in Tables I and II. The parameter T_c^* lies within the two-phase region of the pure system, and the exponent γ^* is considerably smaller than the susceptibility exponent of the pure system, where $\gamma = 1.24$.

For LW-gel samples, $\alpha(q,T)$ showed little q dependence, while scattering from IBAW-gel samples developed increasing asymmetry between scattering at small and large q as the two-phase boundary of the pure system was approached. Because the IBAW system is characterized by a larger correlation length amplitude, ξ will be larger in these mixtures than in the LW mixtures for comparable temperature differences from the critical. Thus, even though the gel-mesh size is roughly the same, the fact that these effects are more obvious in the IBAW system is not surprising. Figure 10 shows $\alpha(q,T)$ for the IBAW-gel sample containing 27 wt.% IBA as calculated from the results shown in Fig. 6. Neutron-scattering studies [29] show that the asymmetry becomes even more pronounced at larger q.

The fact that $\alpha(q,T)$ decreases with increasing q near the critical point can be understood qualitatively as follows. The *linear* response of a critical system to a small field $\delta h(\vec{q})$, which varies sinusoidally in space, is not independent of the wave vector of the field; instead, the response is described rather accurately by the Ornstein-Zernike result,

$$\delta c(\vec{q}) = \frac{\delta h(\vec{q})\,\chi}{1+q^2\xi^2} \quad , \tag{13}$$

where χ is the susceptibility and ξ is the correlation length of the critical system. Thus, as the critical point is approached and ξ grows to the point where $q\xi$ is no longer small compared to unity, the response of the concentration to the higher wave vector components of the field due to the silica should be less than the response at low wave vector. This is consistent with the data of Fig. 10; however, the q dependence indicated in Eq. (13) does not accurately fit the data. Recent neutron-scattering results [29] do show good agreement with this q dependence far from the critical temperature of the pure system, with slight residuals as the two-phase boundary of the pure system is approached. The non-Ornstein/Zernike q dependence, together with the failure of $\alpha(q=0,T)+\bar{\phi}_a^{mixt}$ to diverge as strongly as χ, indicate that the overall response of the mixture to the gel is not linear.

3. *Dual-region model*

A qualitative reason for the differences between samples apparent in Fig. 8 lies in the effect critical adsorption of one component has on the concentration of the remaining, nonadsorbed fluid, together with the fact that the behavior of a critical fluid mixture depends quite strongly

TABLE I. Results of fitting $\alpha(q=0,T)$ for LW gels of various concentrations to the equation $\alpha(q=0,T)+\bar{\phi}_l^{mixt}=\alpha_0(T_c^*-T)^{-\gamma^*}$.

wt.% lutidine	$\bar{\phi}_l^{mixt}$	α_0	T_c^*(°C)	γ^*
21	0.24	12.43±0.5	38.6±0.2	0.65±0.01
26	0.29	9.66±0.06	36.5±0.2	0.68±0.02
31	0.31	4.36±0.2	34.02±0.09	0.51±0.02
34	0.34	3.39±0.02	33.45±0.02	0.426±0.003
37	0.37	2.37±0.06	34.1±0.1	0.37±0.01
41	0.41	1.93±0.04	35.9±0.1	0.327±0.007

TABLE II. Results of fitting $\alpha(q = 0, T)$ for IBAW gels of various concentrations to the equation $\alpha(q = 0, T) + \bar{\phi}_w^{mixt} = \alpha_0 (T - T_c^*)^{-\gamma^*}$.

wt.% IBA	$\bar{\phi}_w^{mixt}$	α_0	T_c^* (°C)	γ^*
26	0.73	1.90±0.04	25.5±0.1	0.27±0.01
27	0.71	2.71±0.09	27.0±0.1	0.33±0.02
28	0.69	3.09±0.30	27.2±0.4	0.35±0.04

on both concentration and temperature near the consolute point. To discuss this effect, we arbitrarily divide the fluid into two regions, one containing "adsorbed" fluid and the other containing "free" fluid. Although we cannot deduce the volumes occupied by the adsorbed fluid or the remaining free fluid, we can use the data for $\alpha(q = 0, T)$ to estimate [32] the average volume fraction of the preferentially attracted species in the free, nonadsorbed fluid, which we denote as $\bar{\phi}_a^{free}$. We model the adsorbed fluid as occupying a fraction of the sample volume $\phi^{ad}(\vec{r})$, which depends on position in the sample, and which is proportional to the volume of the sample locally occupied by silica,

$$\phi^{ad}(\vec{r}) = \beta \, \phi_s(\vec{r}) \quad . \tag{14}$$

The volume fraction of preferentially attracted species in the adsorbed fluid is denoted ϕ_a^{ad}, and conservation of the preferentially attracted species leads to an expression for the local concentration of this species

$$\begin{aligned} \phi_a(\vec{r}) &= \phi_a^{ad} \, \phi^{ad}(\vec{r}) + \phi_a^{free} \, [1 - \phi^{ad}(\vec{r}) - \phi_s(\vec{r})] \\ &= \phi_a^{ad} \, \beta\phi_s(\vec{r}) + \phi_a^{free}[1 - (1 + \beta) \, \phi_s(\vec{r})] \quad . \end{aligned} \tag{15}$$

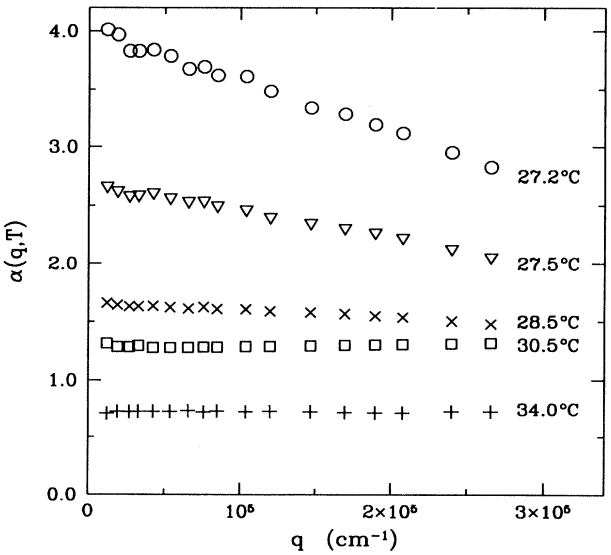

FIG. 10. The response function $\alpha(q, T)$ as determined from the data shown in Fig. 6 using Eq. (10). The q dependence of α becomes more pronounced as the two-phase boundary of the pure system is approached. The temperatures at which the measurements were made are shown next to each data set.

Neglecting any variation in ϕ_a^{ad} or ϕ_a^{free} with position, the fluctuations in the preferentially attracted species are given by

$$\delta\phi_a = \bar{\phi}_a^{ad} \beta \delta\phi_s - \bar{\phi}_a^{free}(1 + \beta)\delta\phi_s \quad . \tag{16}$$

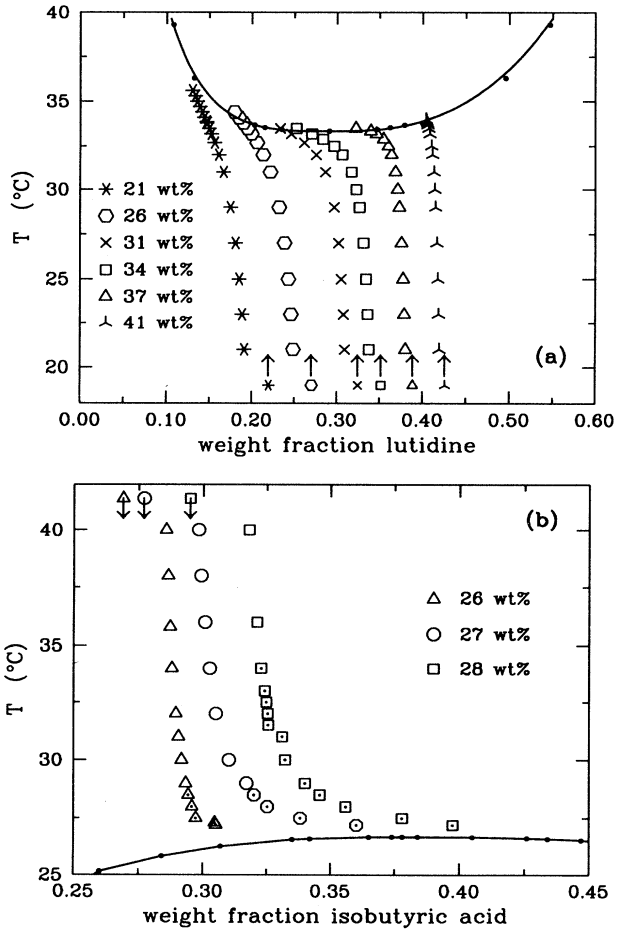

FIG. 11. Effect of adsorption on the concentration of the free fluid as calculated using Eq. (18). The gels are all 4 wt.% silica and have crossover lengths of about 300 Å. The concentration of the free fluid is shifted quite dramatically as the critical point is approached. The solid curves are measurements of the coexistence curve for the pure systems. (a) Weight fraction of lutidine in the free fluid vs temperature for LW-gel samples of various lutidine concentrations. (b) Weight fraction of IBA in the free fluid vs temperature for IBAW-gel samples of various isobutyric acid concentrations. The symbols with arrows far away from the coexistence curve in parts (a) and (b) indicate the average concentration of lutidine and isobutyric acid, respectively, averaged over the mixture $\bar{\phi}^{mixt}$.

Recalling the definition of α as expressed in Eq. (9), we find

$$\alpha = \beta\bar{\phi}_a^{ad} - (1+\beta)\bar{\phi}_a^{free} \quad . \tag{17}$$

Solving for β, using Eq. (15), and averaging over the sample, we finally obtain a very simple result for the average concentration of the preferentially attracted species *in the free fluid*,

$$\bar{\phi}_a^{free} = \bar{\phi}_a - \alpha\bar{\phi}_s \quad . \tag{18}$$

In order to estimate the concentration of the free fluid, we use $\alpha(q=0,T)$, which quantifies the response of the fluids to long-wavelength, but small-amplitude, deviations in silica concentration. This result is independent of the volume occupied by the adsorbed layer or its concentration.

Obviously, this model is oversimplified; the fluid volume has been divided into two regions of uniform but distinct concentration when, in reality, the composition must vary smoothly in space. Nevertheless, it serves to demonstrate what must be an important effect; critical adsorption changes the concentration of the remaining free fluid, and the effect becomes quite temperature dependent in the critical region. This is shown by the results for $\bar{\phi}_a^{free}$ obtained as a function of temperature for both LW-gel and IBAW-gel samples of various overall concentrations, as shown in Figs. 11(a) and 11(b). The arrows show the average concentration of the fluid portion of each sample as measured by gas-phase chromatography. Had no adsorption occurred, each sample would have followed a vertical path to the coexistence curve. The figures show a strong shift toward a lower concentration of the adsorbed component as the two-phase boundary of the pure system is approached. The solid curves show measured coexistence curves [36,37], shifted vertically to agree with the critical temperatures that we measured for pure samples.

The effect of adsorption on the concentration of the free fluid provides a qualitative explanation of the behavior of the data for $\alpha(q=0,T)$ shown in Fig. 8. We would expect that samples whose concentration was shifting towards the critical concentration as $T \to T_c$ would show $\alpha(q=0,T)$ diverging faster near the two-phase boundary of the pure system than well away from it, since the susceptibility of a critical system diverges only at the critical point (critical concentration and temperature). Samples whose concentration was shifting away from the critical point should show $\alpha(q=0,T)$ increasing more slowly near the two-phase boundary of the pure system than further away from it. Considering the behavior of the $\alpha(q=0,T)$ data of each sample in regard to the path we have estimated its free fluid to follow in the phase diagram, we find that these two effects are consistent.

B. Dynamics

1. *Analysis of correlation functions*

A pure mixture near the consolute point is characterized by a mass diffusion coefficient which goes strongly to zero at the critical point. This behavior may be studied very accurately using the technique of dynamic light scattering [33]. This technique allows one to measure the temporal autocorrelation function for the thermally induced concentration fluctuations, since the scattered field is proportional to the concentration fluctuation of the same wave vector $\vec{q}$. The normalized autocorrelation function for the scattered field amplitude $g^{(1)}(\tau)$ is defined as

$$g^{(1)}(\tau) \equiv \frac{\langle E(q,\tau)E^*(q,0)\rangle}{\langle |E(q)|^2\rangle} = \frac{\langle \delta\phi(q,\tau)\delta\phi^*(q,0)\rangle}{\langle |\delta\phi(q)|^2\rangle} \quad . \tag{19}$$

For a pure mixture, the fluctuations relax exponentially in time to quite high accuracy. The relaxation rate $\Gamma(q)$ defines the wave-vector-dependent diffusion coefficient $D(q)$,

$$g^{(1)}(\tau) = e^{-\Gamma(q)\tau} = e^{-D(q)q^2\tau} \quad . \tag{20}$$

In the $q=0$ limit, $D(q)$ is equal to the diffusion coefficient, which would be measured macroscopically. It is directly related to the correlation length of the spontaneous fluctuations ξ, which diverges at the critical point. The relationship between $D(q=0)$ and ξ is accurately given by [34,35]

$$D(q=0) = \frac{k_B T}{6\pi\eta\xi} \quad , \tag{21}$$

where η is the viscosity of the mixture, which diverges, but only very weakly.

Dynamic light-scattering studies of various LW-gel samples did not reveal any temporal fluctuations. The sensitivity of these measurements was such that fluctuations at 15% of the level displayed by pure mixtures within 0.5 °C of T_c should have been detected. On the other hand, dynamic measurements of the IBAW-gel samples did show temporal fluctuations, although the amplitude of the dynamic signal relative to the baseline was lower than it was for pure samples. In fact, rotating the sample to different orientations resulted in different amplitudes and apparently different decay rates. By direct visual observation of the samples, it was clear that a significant fraction of the scattering consisted of a static, time-independent speckle field. At the same time, measurement of the intensity-intensity correlation function showed that a fraction of the scattered light was time dependent. Generally, the ratio of signal amplitude to baseline was largest when the static scattering was at a minimum and decreased as the static scattering increased, *but this was not always the case.* This situation is an excellent example of light scattering from a nonergodic system [38]. The system is nonergodic in the sense that for any given position and orientation of the sample relative to the incident beam and collection optics, the scattered field corresponds to only a single realization of the time-independent speckle field. Time averaging will allow measurement of the average properties (amplitude

and correlation function) of the time-dependent speckle field, but not those of the time-independent speckle field.

Under these conditions light scattering can be used to deduce both the intensity of the fluctuating component of the scattered light, as well as its temporal autocorrelation function, but considerable care must be taken in the data analysis.

This situation is most profitably analyzed in terms of the amplitude of the scattered electric field rather than the intensity. Thus we write the scattered field amplitude $E(t)$

$$E(t) = E_s + E_f(t) \tag{22}$$

in terms of a static component E_s and a fluctuating component E_f. The fluctuating component at any given spatial location in the far field is taken to be a zero-mean complex Gaussian random process, since it results from the fields scattered by many independent sources. The static field is a single sample of such a process. Both field components exhibit the same spatial correlation (they are speckle fields) because they both originate from the same illuminated volume which is of finite dimension.

A digital autocorrelator measures the quantity $\langle n(t)n(t+\tau)\rangle/\langle n(t)\rangle^2$ for various delay times τ. Here, $n(t)$ is the number of photomultiplier tube output pulses detected during a period of time centered on time t. This autocorrelation function is an excellent measure of the intensity-intensity autocorrelation function $G^{(2)}(\tau)$, where

$$G^{(2)}(\tau) = \langle I(t)\ I(t+\tau)\rangle \quad . \tag{23}$$

An experiment carried out with the sample fixed in orientation and position results in a measurement of $G^{(2)}(\tau)$ for one particular representation of the static speckle field, regardless of how long the experiment is run. We denote such a correlation function, measured at a single spatial point in the far field as $G_j^{(2)}(\tau)$, referring to the particular representation by the subscript j. Defining $I_f \equiv \langle E_f(t)\ E_f^*(t)\rangle$ (where angular brackets denote time averaging) and $I_{sj} = E_{sj}\ E_{sj}^*$, it is straightforward to obtain

$$G_j^{(2)}(\tau) = I_j^2 + \left\{ 2\, I_{sj}\, I_f\, g_f^{(1)}(\tau) + I_f^2 \left[g_f^{(1)}(\tau) \right]^2 \right\} \quad , \tag{24}$$

where $g_f^{(1)}(\tau) = \langle E_f(t)\ E_f^*(t+\tau)\rangle / I_f$ is the normalized field-field correlation function for the fluctuating component of the scattered field amplitude, and $I_j = I_{sj} + I_f$. Physically, the term linear in $g_f^{(1)}$ is the result of the time-dependent field mixing with the time-independent field while the $[g_f^{(1)}]^2$ term is the result of it mixing with itself. Note that $g_f^{(1)}(\tau)$ is independent of the realization of the static speckle field present during the measurement. Furthermore, it is precisely $g_f^{(1)}(\tau)$ which contains information regarding the critical order-parameter fluctuations, and which is normally deduced directly from measurements of $G^{(2)}(\tau)$ for ergodic systems. Consequently, it should not be necessary to invoke an involved analysis in order to deduce $g_f^{(1)}(\tau)$ from even a single measurement of $G_j^{(2)}(\tau)$. Instead, one may fit the data for any particular $G_j^{(2)}(\tau)$, using Eq. (24), provided that a functional form is available for $g_f^{(1)}(\tau)$. In doing this, the parameter I_f must be adjusted in addition to any parameters involved in $g_f^{(1)}(\tau)$, but I_{sj} is constrained by knowing $I_j = I_{sj} + I_f$, which can easily be measured almost exactly for any given representation by noting the average count rate. A further advantage of this method of analysis is that one obtains the physically interesting quantity I_f, which is the mean-squared amplitude of the fluctuating field component.

To demonstrate the effect of changing the sample orientation, and thus the static scattering contribution, Fig. 12 shows the decaying portion of the normalized intensity-intensity correlation function $g^{(2)}(\tau)$ for the 27 wt.% IBA sample measured at 40 °C (far from T_c) with $q = 1.9 \times 10^5$ cm^{-1} and with the sample held in several different orientations. Each measurement resulted from a different realization of the static speckle field. Each measured correlation function has been scaled by its own baseline, and only the decaying portions are shown. Not only are the scaled amplitudes of the three data sets quite different, but the relative amplitudes of the $g_f^{(1)}$ and $[g_f^{(1)}]^2$ terms differ as well. For these three data sets, the amplitude to baseline ratios were 0.083, 0.049, and 0.026, while the ratios of I_f to I_{sj} were 0.064, 0.036, and 0.0182, respectively. When the individual correlation functions were fitted using Eq. (24), with a single exponential form for $g_f{}^{(1)}(\tau)$, the fits were all excellent, as shown by the solid lines in the figure, but the results for the parameter I_f showed deviations of order ±5%. The results for the decay rate, however, were much better defined, showing deviations of only ±1%.

We speculate that the variations in I_f occurred because the effective center of curvature of the static speckle field, for any particular orientation of the sample, can lie any-

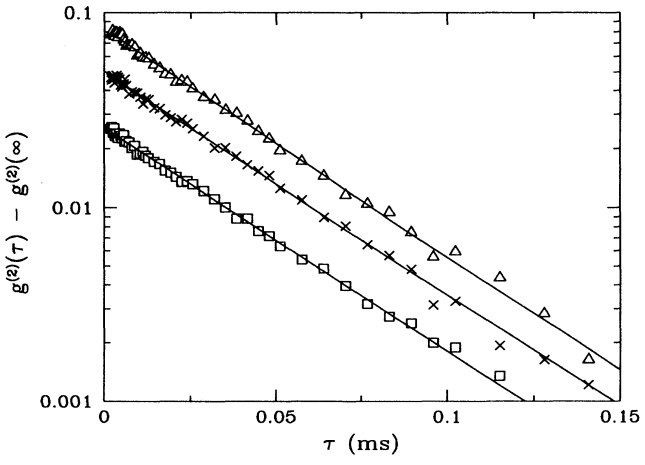

FIG. 12. Time correlation functions measured for the sample containing 27 wt.% IBA at 40 °C and at $q = 1.90 \times 10^5$ cm^{-1}. The different amplitudes resulted from taking data at different sample orientations. The solid curves are fits to Eq. (24) using a single exponential form for $g_f{}^{(1)}(\tau)$.

where within the volume from which scattered light is collected, while the time-dependent pattern has, on average, a center of curvature lying at the center of the collection volume. That is to say, different static speckle pattern realizations result in different degrees of wavefront mismatch between the static and fluctuating field components averaged over the finite collection aperture, even after time averaging over a large number of realizations of the fluctuating speckle field. The parameter I_f is directly sensitive to the mixing efficiency of the static and fluctuating fields, whereas the decay rate is independent of it. This effect was very serious when data were taken using larger apertures (ranging from 1.0 to 2.2 mm) which resulted in amplitude to baseline ratios of $\simeq 0.15$ for the pure system. It was to reduce these unwanted deviations in the results obtained for I_f that we reduced the aperture diameters to 0.34 mm, so as to approach point detection and perfect mixing efficiency more closely.

This observation raises the issue of how to properly analyze dynamic light scattering data obtained for the gel-mixture system using finite diameter collection apertures. We reasoned that the static speckle field is the result of sampling a zero-mean complex Gaussian random process with exactly the same spatial coherence properties as the fluctuating field. Had it not been static, but instead allowed to evolve in time, dynamic light-scattering data taken with a finite aperture diameter would contain three decaying terms and would be given by

$$G^{(2)}(\tau) = (I_s + I_f)^2 + \beta\Big\{ {I_s}^2 \left[g_s^{(1)}(\tau)\right]^2 + 2\, I_s\, I_f \left[g_s^{(1)}(\tau)\right]\left[g_f^{(1)}(\tau)\right] + I_f^2 \left[g_f^{(1)}(\tau)\right]^2 \Big\} \quad . \tag{25}$$

Here, $I_s \equiv \langle E_s(t) E_s{}^*(t)\rangle$, is the time average for the previously static field, which we now imagine to be fluctuating slowly, and $g_s^{(1)}(\tau)$ is the normalized field-field correlation function for that process. The geometrical factor β is related to the number of coherence areas detected. Note that the factor $\beta \leq 1.0$ is identical for all three decaying terms. This is a well known result for scattering from a mixture of two species that have different correlation functions, ${g_s}^{(1)}(\tau)$, and ${g_f}^{(1)}(\tau)$. For samples where the slow fluctuations are actually static, such a measurement can be approximated by averaging correlation functions corresponding to various representations of the static speckle field. This was done by making measurements of $G_j^{(2)}(\tau)$, as defined in Eq. (24), for a number of different orientations of the sample. We denote this average correlation function by $G_{avg}^{(2)}(\tau)$. It is given by

$$G_{avg}^{(2)}(\tau) = \langle (I_s + I_f)^2 \rangle_{avg} + \beta\Big\{ 2\,\langle I_s\rangle_{avg}\, I_f \left[g_f^{(1)}(\tau)\right] + I_f^2 \left[g_f^{(1)}(\tau)\right]^2 \Big\} \quad , \tag{26}$$

and in normalized form by

$$g^{(2)}{}_{avg}(\tau) = 1 + \beta\Big\{ \frac{2\,\langle I_s\rangle_{avg}\, I_f}{\langle (I_s + I_f)^2\rangle_{avg}} \left[g_f^{(1)}(\tau)\right] + \frac{{I_f}^2}{\langle (I_s + I_f)^2\rangle_{avg}} \left[g_f^{(1)}(\tau)\right]^2 \Big\} \quad , \tag{27}$$

where $\langle\ \rangle_{avg}$ denotes the average over the set of measurements. Note that this correlation function has a baseline given by $\langle (I_s + I_f)^2\rangle_{avg}$, and not by $\langle I_s + I_f\rangle_{avg}^2$. A baseline value of $\langle I_s + I_f\rangle_{avg}^2$ is obtained only when both fields fluctuate, and the correlation function is measured for values of the delay time τ large enough for both $g_s^{(1)}(\tau)$ and $g_f^{(1)}(\tau)$ to have decayed completely to zero [see Eq. (25)].

In practice, we found that we could determine both I_f and $g_f^{(1)}(\tau)$ quite well by measuring $G_j^{(2)}(\tau)$ for ten different orientations of the sample and averaging them to obtain an experimental result for $G_{avg}^{(2)}(\tau)$. In doing this we measured each individual $G_j^{(2)}(\tau)$ for essentially the same time. Since the correlator we used provides results for the normalized correlation function $g_j^{(2)}(\tau)$, we calculated $G_j^{(2)}(\tau)$ for each measurement by multiplying the measured $g_j^{(2)}(\tau)$ by I_j^2. We used the total number of photocounts received by the correlator during the jth measurement as our measure of I_j. Figure 13 shows a normalized average correlation function $g_{avg}^{(2)}(\tau)$ obtained in this way for the 27 wt.% IBAW-gel sample at a temperature of 40 °C and a scattering wave vector of $q = 1.9 \times 10^5$ cm^{-1}. The averaged correlation function is fit to Eq. (27), with $g_f^{(1)}(\tau) = e^{-\Gamma\tau}$, and the fit

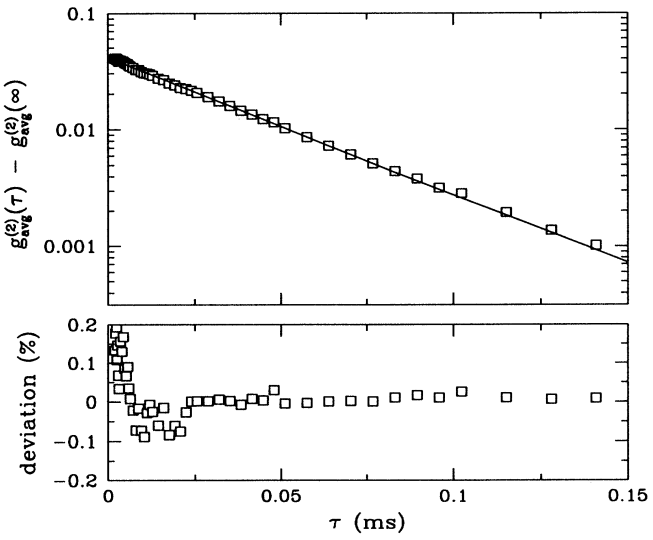

FIG. 13. Normalized average autocorrelation function measured using ten different orientations for the sample containing 27 wt.% IBA at 40 °C and at $q = 1.90 \times 10^5$ cm^{-1}. The solid curve is a fit to Eq. (27) using a single exponential form for ${g_f}^{(1)}(\tau)$. The lower graph shows the deviation of the fit from the data, expressed as a percentage of the data.

is shown by the solid line. The parameter β depends on the optical geometry and was determined independently for each scattering angle from measurements of the amplitude of the temporal autocorrelation function of pure mixtures, for which the scattered field amplitude contains no static term. We also found that accurate data could be obtained by rotating the gel while measuring the correlation function, provided the rotation rate was sufficiently slow compared to all relaxation rates in the system; however, we did not use this method. The values for I_f were used to obtain the fluctuating portion of the scattered intensity that was subtracted from the total scattered intensity when determining $\alpha(q,T)$.

2. *Time-dependence of fluctuations*

These measurements revealed three dynamic regimes for the IBAW-gel system. Far from the two-phase boundary of the pure system, the concentration fluctuations exhibited exponential relaxation [open symbols in Fig. 11(b)]. The dynamics crossed over to a nonexponential form [symbols with a dot at the center in Fig. 11(b)] as the two-phase boundary of the pure system was approached. Figure 14 shows averaged correlation functions for the 27 wt.% sample at various temperatures with $q = 1.9 \times 10^5$ cm^{-1} and corresponding fits, obtained as described below. The data are least accurately exponential at larger values of the scattering wave vector q, but remain exponential and diffusive (decay rate $\propto q^2$) at sufficiently small q. When the temperature was decreased to within ~ 0.5 °C of the pure system's coexistence curve, the dynamics abruptly developed an extra, very slow, component. Correlation functions (not averaged) measured in this regime are shown in Fig. 15. The

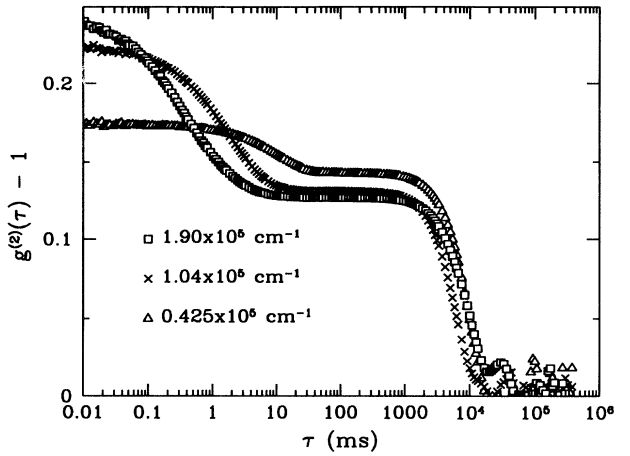

FIG. 15. Time correlation functions measured in the sample containing 27 wt.% IBA at 27.05 °C at several scattering wave vectors showing slow dynamics as well as the faster nonexponential dynamics of Eq. (29).

decay rate associated with this slow mode appeared to be roughly q independent.

The data in the first two dynamic regimes are consistent with either of two forms for $g_f^{(1)}(\tau)$,

$$g_f^{(1)}(\tau) = A_1 \exp[-\Gamma_1 \tau] + A_2 \exp[-(\Gamma_2 \tau)^x] \quad , \qquad (28)$$

or

$$g_f^{(1)}(\tau) = A_1 \exp[-\Gamma_1 \tau] + A_2 \times \exp\left[-\left(\frac{\ln(\tau/t_0)}{\ln(\Gamma_2^{-1}/t_0)}\right)^3\right] \quad . \qquad (29)$$

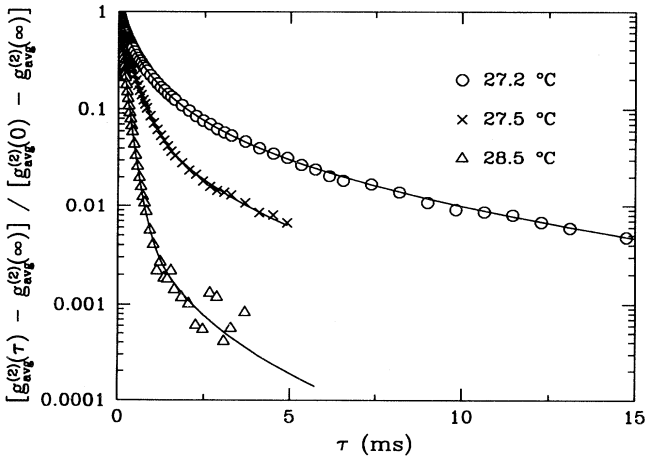

FIG. 14. Normalized average autocorrelation functions for the sample containing 27 wt.% IBA at $q = 1.90 \times 10^5$ cm^{-1} at temperatures of 28.5, 27.5, and 27.2 °C approaching the two-phase boundary of the pure system together with fits to Eqs. (27) and (29) with $A_2 = 0.12$, 0.46, and 0.85, respectively. Each correlation function is the result of averaging of ten measurements.

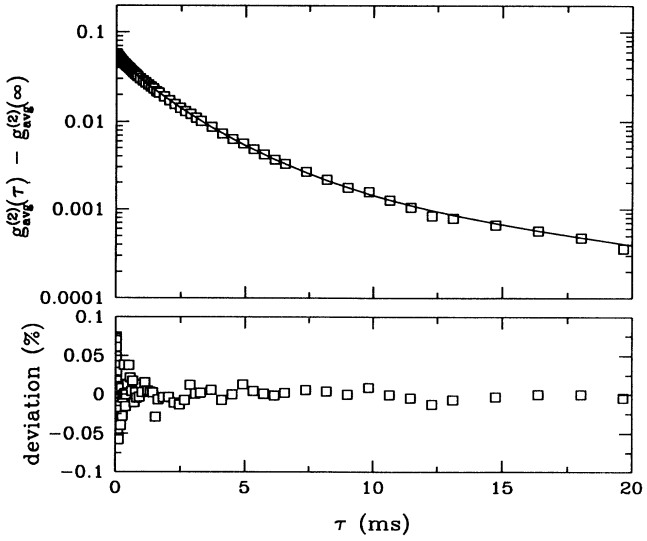

FIG. 16. Average correlation functions measured using ten orientations of the sample containing 27 wt.% IBA at $q = 1.04 \times 10^5$ cm^{-1} at 27.2 °C together with the fit to Eqs. (27) and (29). The lower graph shows the deviation of the fit from the data, expressed as a percentage of the data.

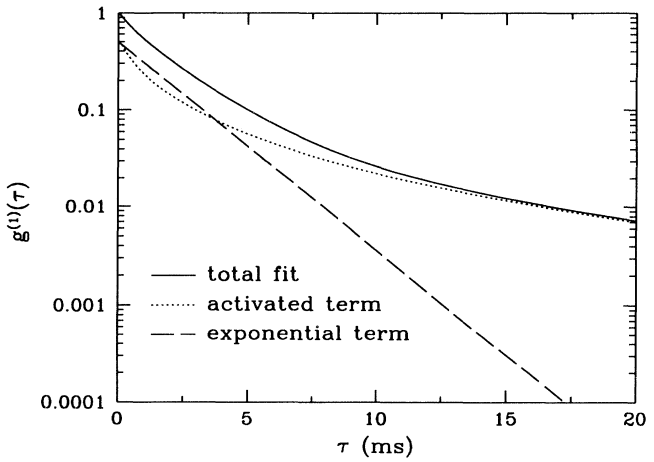

FIG. 17. Relative contributions of the two terms in the field-field correlation function $g_f^{(1)}$, used to fit the data shown in Fig. 16. The solid curve shows the total correlation function, the dashed curve shows the single exponential contribution, and the dotted curve shows the contribution of the activated term.

In both cases, the fits were made with the constraint [39] that $A_1 + A_2 = 1$. The first form includes a stretched exponential [40] that is purely empirical, and the second term of Eq. (29) is predicted by activated dynamic scaling theory [9] and has been used to fit Monte Carlo simulations of random-field systems [41] and light-scattering data of binary fluids in Vycor [11]. Both forms fit well, and results for the parameters A_1, Γ_1, and Γ_2 were consistent for the two fits, but the second typically gave a smaller χ^2; the results of this fit will be reported here. Note, however, that the assumptions made in dynamic scaling arguments may not apply here. In particular, the assumption that the correlation length has grown to contain many random-field sites may not be relevant. For the temperature range in which the second term of $g_f^{(1)}(\tau)$

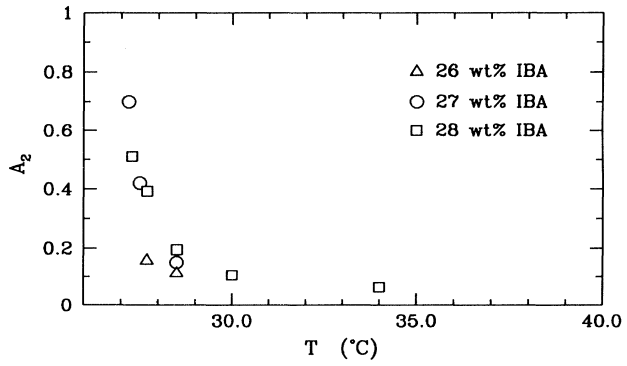

FIG. 18. Behavior of the amplitude of the nonexponential term in the field-field correlation function [Eq. (29)] at high q (2.65×10^5 cm^{-1}) as the two-phase boundary of the pure system is approached for IBAW-gel samples containing 26, 27, and 28 wt.% IBA.

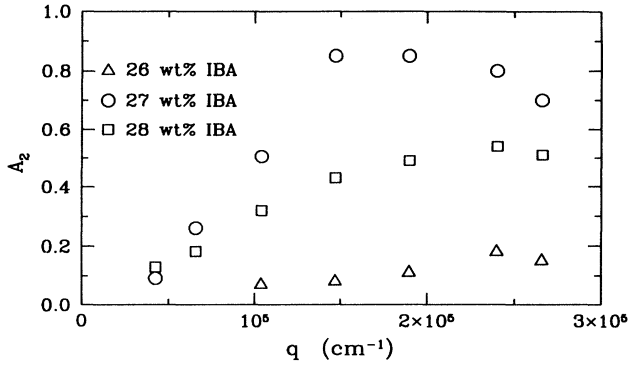

FIG. 19. Dependence of the amplitude of the nonexponential term in the field-field correlation function [Eq. (29)] on q for temperatures above those corresponding to the onset of slow dynamics for IBAW-gel samples containing 26, 27, and 28 wt.% IBA at temperatures of 27.7, 27.2, and 27.3 °C, respectively.

is significant, the correlation length [as calculated from Eq. (21)] is smaller than the crossover length of the gel. Figure 16 shows an example of averaged data for the intensity-intensity correlation function and the fit (solid curve) using Eqs. (27) and (29) for the 27 wt.% sample at 27.2 °C and $q = 1.04\times10^5$ cm^{-1}. Figure 17 shows the relative contributions to the field-field correlation function $g_f^{(1)}$ for the fit shown in Fig. 16; the dashed curve is the single exponential, the dotted curve shows the contribution from the activated term, and the solid curve shows the sum.

Well above the phase boundary of the pure mixture, the correlation function was exponential with $A_1 \simeq 1$. Closer to the phase boundary, the amplitude A_2 of the activated term increased. Figure 18 shows the temperature dependence of A_2 at the largest q measured (2.65×10^5 cm^{-1}) for the three different samples. The fits could not determine $A_2 < 0.1$. We attribute the sample-to-sample variation of the temperature at which the dynamics first became noticeably nonexponential to the fact that the gel for the 27 wt.% sample came from a different batch than did those for the other two samples, and it had a slightly smaller crossover length. Figure 19 shows the q dependence of A_2 at temperatures ~ 0.1 °C above where the slow dynamics regime begins for each of the three samples; the amplitude is larger at large q with possibly a slight maximum vs q. The fact that the decay of the correlation function becomes exponential in the $q = 0$ limit means that a long-wavelength disturbance of the concentration away from its average value result in a concentration flux which is linear in the concentration disturbance (Fick's law). The nonmonotonic behavior of A_2 as a function of q for the 27 wt.% sample is surprising; we have no explanation for it.

Results obtained for Γ_1/q^2 for several temperatures for the 27 wt.% sample are shown in Fig. 20. We observed that $\Gamma_1 \propto q^2$ for all of the temperatures and samples studied. This is the hallmark of a diffusive process, with a diffusion coefficient $D = \Gamma_1/q^2$. It is clear from the figure that D decreases as the critical region is approached.

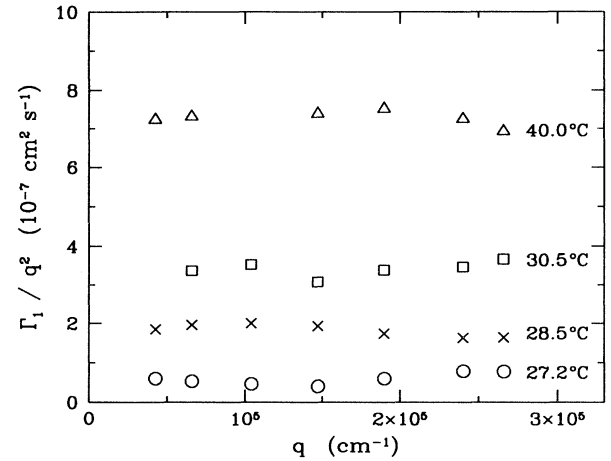

FIG. 20. Γ_1/q^2 as a function of q at temperatures of 40 (△), 30.5 (□), 28.5 (×), and 27.2 °C (○) for 4.0 wt.% silica gel containing 27 wt.% IBA. Γ_1/q^2 is essentially independent of q as it is for the pure mixture, when $q\xi < 1$.

We have analyzed our data so as to extract D for each sample at each temperature studied. Figure 21(a) shows the ratio of the diffusion coefficient measured in the gel-mixture system to that of pure mixtures at the same temperature and having a concentration equal to the *average concentration of the mixture in the gel.* Values for the pure mixtures were obtained from the data shown in Fig. 3. The diffusion coefficients measured in the gel-mixture system are consistently smaller than those of the pure mixture at the same temperature and average concentration.

There are at least two possible explanations for this observation. It is qualitatively consistent with screening of hydrodynamic flow by the gel strands, which would result in enhanced drag and a smaller diffusion coefficient. Alternatively, the diffusion coefficients vary in a way reasonably consistent with what would be expected considering the behavior of the concentration of the free fluid shown in Fig. 11(b). For example, at the temperatures closest to the coexistence curve of the pure system, the diffusion coefficients are 1.42×10^{-7}, 0.593×10^{-7}, and 0.810×10^{-7} cm^2/s for the samples containing 26, 27, and 28 wt.% IBA, respectively. The sample that appears to approach closest to the critical point in Fig. 11(b) also has the smallest diffusion coefficient. Figure 21(b) shows the ratio of the diffusion coefficient of each sample to that of the pure mixture at the same temperature and at the *concentration of the free fluid* obtained using Eq. (18). Values for the pure mixture were obtained by interpolation of our data for pure mixtures. Throughout most of the first two dynamic regimes, the diffusion coefficients are nearly equal to those of the pure mixture, deviating significantly only at the lowest temperatures. Close to the coexistence curve of the pure system, the diffusion coefficient of the gel-mixture system is consistently a little larger than that of the pure system at the concentration of the free fluid, although this could be due to slight differences in impurity concentration which can alter the phase-separation temperature.

Figure 22 shows the ratio of Γ_2 to Γ_1 as a function of q for the IBAW gel sample containing 27 wt.% IBA for three temperatures, 28.5, 27.5, and 27.2 °C. The two decay rates, Γ_1 and Γ_2, are quite comparable in both

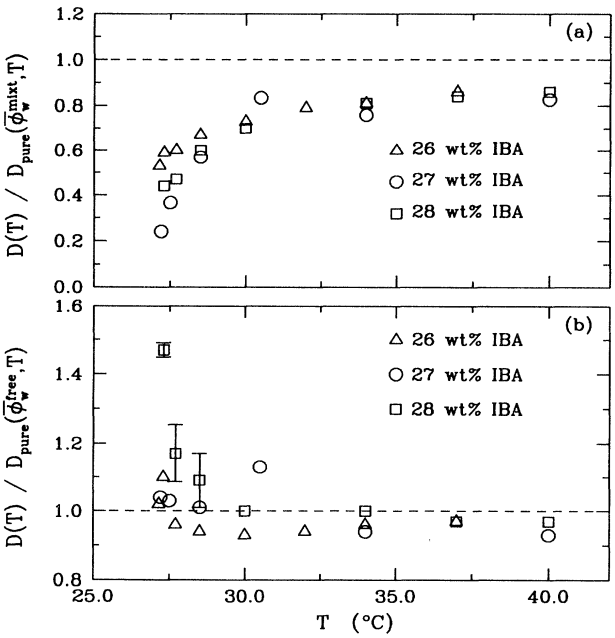

FIG. 21. (a) Ratio of the diffusion coefficient averaged over q for IBAW gel samples containing 4.0 wt.% silica to that of the pure system, at the same temperature and at the average concentration of the mixture in the gel. (b) Ratio of the diffusion coefficient averaged over q for IBAW-gel samples containing 4.0 wt.% silica to that of the pure system, at the same temperature and at the concentration estimated for the free fluid. The error bars show the effect of a ± 1 wt.% error in the estimation of the concentration of IBA in the gel for the measurements most sensitive to this effect.

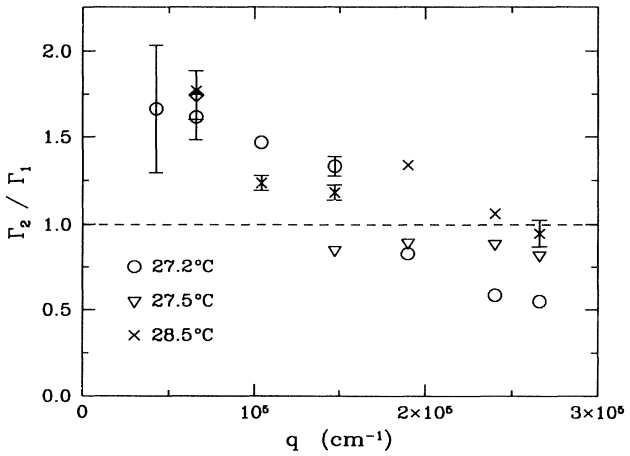

FIG. 22. Ratio of the two decay rates, Γ_2, and Γ_1 as a function of q, for the sample containing 27 wt.% IBA at several temperatures showing that the two decay rates are comparable.

magnitude and q dependence over most of the q and T range studied. The q dependence of the second decay rate Γ_2 was also consistent with diffusive behavior.

3. Intensity of fluctuations

The intensity of the fluctuating component of the scattered light I_f was obtained as a result of fitting the intensity-intensity correlation functions to Eq. (27). Figure 23 shows results for the 27 wt.% IBAW gel sample as a function of q at different temperatures. The results have been corrected for the incident intensity and the gain of the detector. Unfortunately, I_f does not develop enough q dependence in this temperature range to allow accurate extraction of the correlation length of the gel-mixture system from this data. The results for I_f can be compared to the intensity scattered by the pure system at the same temperature and at either the average concentration of the sample or at the concentration of the free fluid. Figure 24(a) shows the q-averaged ratio $I_f/I_{pure}(\bar{\phi}_w^{mixt})$ as a function of temperature for the three samples. This comparison implies that the gel greatly enhances the critical fluctuations of the mixture, which would certainly be an unexpected result. On the other hand, the results are much more reasonable if the intensity is compared to what would be seen in a mixture at the concentration of the free fluid. Figure 24(b) shows the q-averaged ratio $I_f/I_{pure}(\bar{\phi}_w^{free})$; now we see that the amplitude of the time-dependent fluctuations is reduced relative to that of the pure system, i.e., the time-dependent critical fluctuations are suppressed by the gel network. The critical fluctuations are suppressed even at 40 °C, and the suppression becomes stronger as the critical point is approached.

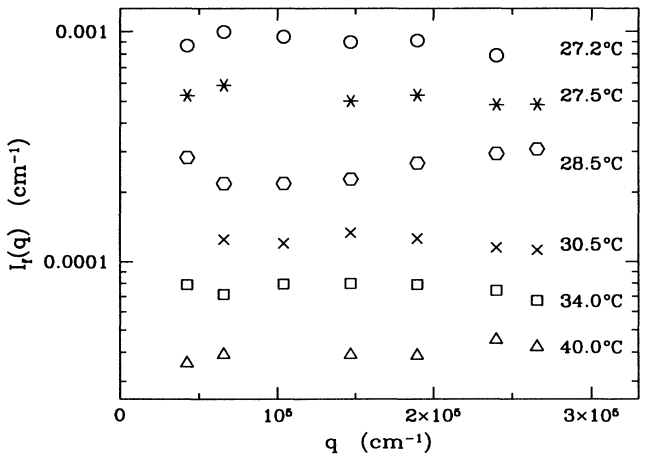

FIG. 23. The intensity scattered by time-dependent fluctuations in the gel-mixture system (27 wt.% IBA) as a function of the scattering wave vector q at various temperatures. The intensity scattered by the fluctuations increases as the two-phase region is approached and is q independent to within the accuracy of these measurements.

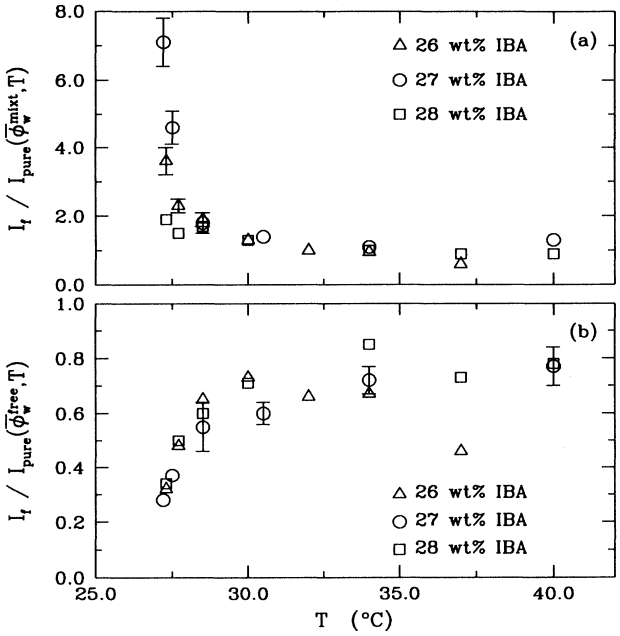

FIG. 24. Temperature dependence of the q-averaged intensity of the time-dependent fluctuations in gel-mixture samples containing various concentrations of isobutyric acid. In (a), the intensity is compared to that of the pure system at the same temperature and at the average concentration of the mixture in the gel. In (b), the intensity is compared to that of the pure system at the same temperature and at the concentration of the free fluid. When not shown, error bars are smaller than the data points.

4. Discussion

The activated form of the dynamics used in Eq. (29) is qualitatively consistent with predictions of Huse [9]. He considered the dynamical properties of the one-phase region of a random-field Ising system with a conserved order parameter. He considered length scales larger than the typical pore size and assumed ξ large enough that the system was in the strong random-field regime where relaxation of concentration fluctuations of size ξ is opposed by free energy barriers scaling like ξ^{ψ} which are large compared to kT. He predicted that, in this regime, the dynamics would be activated with a characteristic relaxation time that would diverge exponentially with ξ as $\ln\tau \sim \xi^{\psi}$ rather than as a power of the correlation length. This behavior should be seen only at shorter length scales, unlike the case of a random field in a nonconserved system where it is seen at all length scales. Over long enough length scales, relaxation would continue to be diffusive because of the conservation constraint placed on the order parameter. The crossover between the two behaviors should occur at some crossover momentum q_x which would vanish exponentially with ξ. For $q_x < q \ll \xi^{-1}$, the correlation function should be the sum of a single exponential and an activated term. In

fact, the functional form of the activated term of Eq. (29) is somewhat empirical. A decay of the form $\exp(-x^p)$ with $x = \ln(t/t_0)$ was predicted, and $p = 3$ was used by Ogielski and Huse [41] to fit Monte Carlo simulations of the three dimensional dilute Ising antiferromagnet in a field. We have observed that p =3, 4, or 5 works equally well in fitting our data. Also, the results for t_0 are not very satisfying; a universal, microscopic result for different q and T was not found. In fact, t_0 varied suspiciously with measurements at different q, frequently being just slightly smaller than the smallest τ included in the fit.

However, our observations differ from these predictions on several points. First, the time scale associated with the activated term seems to be comparable to the diffusive time scale, and there is no evidence for a rapid divergence in the activated time scale. Second, we observe diffusive behavior of this time scale; Huse indicates that the activated time scale should be independent of q.

In this case, it may be appropriate to attribute the modified correlation function to the variety of environments which must be present inside the gel. As fluid is adsorbed, the concentration must vary spatially within the sample. It follows that the local "diffusion coefficient" will also vary spatially. A distribution of relaxation rates is often attributed to correlation functions having the form of Eq. (28).

Our observations of the nature of the temporal correlation function show both similarities to and differences from those seen in measurements of other workers. We find that the correlation function has an exponential form far from the coexistence curve, as would be seen in the pure system. Exponential dynamics far from the coexistence curve was also reported by Xia and Maher [17] (IBAW mixtures in flexible gels) and Dierker and Wiltzius [11] (LW mixtures in Vycor, pore size $\sim$ 70 Å). This behavior was not reported by Wong *et al.* [19] (N_2 in aerogel) and Aliev, Goldburg, and Wu [21] (carbon disulfide-nitromethane mixtures in porous glass, pore size $\sim$ 1000 Å). The lack of this behavior in the latter two works is puzzling, as one would expect the system to approach the behavior of the pure system in the limit where the correlation length is much smaller than the length scale associated with the disorder. In the vapor-liquid systems, it may not be possible to measure the correlation function with standard correlators far enough from T_c to reach this limit, since the time scales are about two orders of magnitude smaller than in fluid mixtures.

As the coexistence curve is approached, we find that the inclusion of a nonexponential correlation function with second correlation time Γ_2 is necessary to fit the data. We find that the diffusion coefficient associated with the exponential portion of the correlation function is comparable to that of the pure system at the concentration of the free fluid except possibly close to the coexistence curve, where it may be a little larger. We find that the second decay rate, Γ_2, is roughly comparable to Γ_1 over most of the q range and temperature range accessible. Samples of lutidine-water mixtures in vycor [11] were found to have an exponential correlation function in the one-phase region of the pure system with a decay rate ($\propto D$) about six times *smaller* than that of the pure system. At $T \sim T_c$, the decay rate for the vycor-mixture system saturated. In these samples, the data only became nonexponential deep into what would be the two-phase region of the pure mixture where the intensity-intensity correlation function was consistent with the sum of two terms, one an exponential form and one a nonexponential, activated form as shown in Eq. (29). The time scale associated with this second term was also much slower than that associated with the exponential term. More recently, this activated decay and associated time scale have been associated with wetting and domain growth [14].

Xia and Maher [17] (IBAW mixtures in gellan gum gels) observed correlation functions that fit a single exponential far from the coexistence curve, and a double exponential as the coexistence curve was approached. The time scale associated with the second exponential was much slower than the first. The second, slower decay could be due to the fact that the samples were immersed in a reservoir, which should lead to slow changes in the concentration as the mean response of the mixture to the gel changes with temperature. In fact, experiments by Aliev, Goldburg, and Wu [21] (carbon disulfide-nitromethane in porous glasses) done in the presence of an external reservoir also exhibit double exponential decay, which the authors attribute to the presence of the reservoir. Experiments done by these authors in the absence of a reservoir exhibit nonexponential decay of the form $G(\tau) \sim (1+x^3)^{-1}$, where $x = ln(\tau/t_\circ)/ln(1/(\Gamma t_\circ))$. They found that the time scale associated with the nonexponential dynamics was much faster, i.e., the diffusion coefficient is larger, than would be seen in the pure system. Wong *et al.* [19] measured correlation functions near the vapor-liquid transition of N_2 in aerogel which showed power law decay $G(\tau) \sim A\tau^{-\phi}$ in the one-phase region of the sample.

An important consideration in comparing these experiments may be the difference in the geometries; for example, vycor is a closed pore glass, while the structure of a gel is much more open. Certainly the fact that the vycor pore diameter is only 70 Å must play a large role in the saturation of Γ near the coexistence curve of the pure fluid. Also, the particular form of nonexponential dynamics observed appears to be sensitive to the structure of the porous material. A second important feature is the presence or absence of a reservoir of fluid; experiments preformed in the presence of a reservoir reveal a second exponential decay while experiments performed without a reservoir are characterized by nonexponential dynamics.

C. Phase separation

For all of the data in Fig. 11, the scattered intensity relaxed monotonically towards equilibrium following any temperature change and equilibrated on a time scale similar to that of the temperature controller ($\sim$10 min). As long as the samples were not exposed to temperatures closer to the phase boundary of the pure systems, the be-

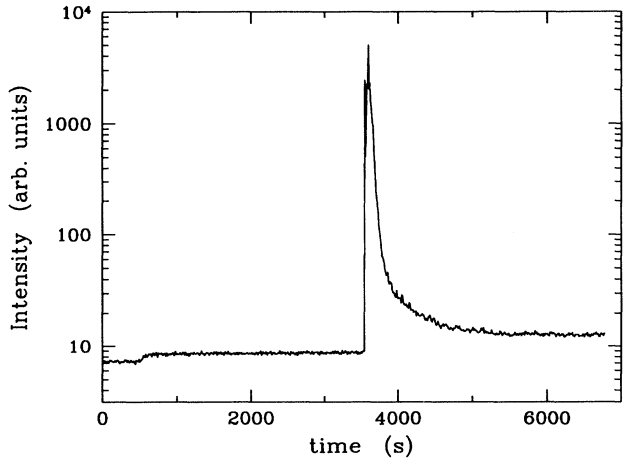

FIG. 25. Change in the scattered intensity (at $q = 1.89\times10^4$ cm^{-1}) following two temperature steps. At around 600 s, the intensity equilibrated promptly following a temperature increase from 33.4 to 33.5 °C. At around 3600 s, a large overshoot in the intensity was observed following a temperature increase from 33.5 to 33.6 °C.

havior of the sample was independent of sample history. For temperatures closer to the phase boundary of the pure system than those shown in Fig. 11 and within the two-phase region of the pure system, the scattered intensity was characterized by overshoots and hysteresis and, for the IBAW-gel samples, a change in the dynamical behavior. For example, Fig. 25 shows the change in intensity observed on heating the LW-gel sample containing 4 wt.% silica and 34 wt.% lutidine. About 600 s into the measurement the temperature was increased from 33.4 to 33.5 °C; the intensity increased monotonically and equilibrated quickly following this change. At around 3600 s, the temperature was increased from 33.5 to 33.6 °C. The intensity quickly increased by over two orders of magnitude, and then decayed slowly (over the course of about 1 h) to a value about twice as large as that measured before the temperature change. The intensity would typically continue to drift slowly for about 24 h after such a temperature change. Similar overshoots were observed in all LW- and IBAW-gel samples whose average concentration was on the side of the coexistence curve rich in the preferentially attracted species. Overshoots were observed only as the system was taken further into the two-phase region of the pure system, never on leaving it. These slow intensity changes meant that samples quenched into the two-phase region of the pure system and then returned to the one-phase region would exhibit behavior that depended on the sample's history while they were returning to equilibrium at a given temperature. In the IBAW-gel samples, a change in the dynamic behavior was observed when overshoots and hysteresis were present. The change in dynamic behavior involved the addition of an extra, slow component with a decay time of about 10 s to the correlation function, while the faster component described by Eq. (29) remained; this behavior is illustrated in Fig. 15. This figure also shows that the characteristic relaxation time of the slow component appears to be q independent. This component died away in amplitude over a time scale of the order of 10 h. If a sample was left in a region where the extra slow component of the dynamics was present for a period of the order of a day and then returned to the one-phase region, the sample took days to return to its previous state, as judged by measurement of $S(q)$.

We associate this behavior with phase-separation of the mixture inside the gel. The overshoots would then correspond to the nucleation and coarsening of small droplets of the minority phase and the hysteresis is consistent with phase-separation on length scales of $\mathcal{O}$(mm). Samples with average concentrations on the side of the coexistence curve rich in the nonattracted species would be expected to show heterogeneous nucleation of the phase rich in the preferentially attracted species and overshoots associated with droplet formation and coarsening would not be expected in this case. Phase separation on length scales comparable to the sample size also occurred. We have observed a deeply quenched sample that became clear in ~6 months, and which had a well defined meniscus between the top and bottom portions of the sample. This shows that these samples macroscopically order, even in the presence of the gel network.

For the IBAW-gel samples, this change in behavior occurred at temperatures about 0.5 °C above the coexistence curve observed for the pure mixture, while the diffusion coefficients were still finite and comparable to what would be seen in a pure system a similar distance from the critical temperature and concentration. This early phase separation could be the result of impurities that can shift the critical temperature. Studies to determine whether this early phase-separation could be an impurity effect are underway, but estimates of the magnitude of the problem are not consistent with the increased phase-separation temperature. As a result of the gelation process, the gels contain some impurities, namely, about 8.5 wt.% methanol and about 0.005M NaCl. Assuming that the impurities diffuse out of the gel as the mixture diffuses in and are diluted as the mixture is refreshed, we estimate that the net effect of these impurities would be a depression of T_c by 0.13 °C. Not only is this change in T_c smaller than that observed, it is also of the wrong sign. Gas chromatography results show the concentration of methanol in the samples to be less than 0.01%, which would lead to a T_c depression of only 0.04 °C. However, unreacted TMOS might also be present.

However, even if some impurity does indeed cause an upward shift in the phase-separation temperature, the anomalous behavior of the diffusion coefficient and associated location of the critical point remain a mystery. If the critical temperatures of our gel-mixture samples are shifted upward by impurities, the ratio of the diffusion coefficient of the gel-mixture system to that of the pure mixture would be even larger than that which is apparent in Fig. 21(b); the diffusion coefficient of the gel-mixture system would then be appreciably larger than that of the pure system near the coexistence curve. We believe that the concentrations of the free fluid in the gel-mixture samples studied have come within 1 wt.% of the

critical concentration of the pure system near the critical temperature. Our analysis of α and estimates of the free-fluid concentration indicate that some of the samples appear to phase separate with $\bar{\phi}_w^{free}$ on the IBA-rich side of the coexistence curve, and others appear to phase separate with it on the W-rich side of the coexistence curve. However, there is no indication that the diffusion coefficient goes to zero as it does at a consolute critical point. Apparently, the system phase separates before this can happen.

At the temperatures for which phase-separation occurs, the correlation length, as estimated from the diffusion coefficients using Eq. (21), is of the order of half the crossover length of the gel. (Unfortunately, we were not able to extract the correlation length of the gel-mixture system directly from measurements of the fluctuation part of the scattered intensity.) Presumably, the concentration in the gel changes significantly over length scales of the order of the crossover length of the gel in order to satisfy the requirement that the overall concentration of the mixture within the sample be fixed. Such gradients in concentration become increasingly important relative to other terms in the free energy as the critical point is approached, and presumably could have a strong effect on determining when the system will separate into two phases of different concentrations.

IV. SUMMARY AND CONCLUSIONS

We have used light-scattering measurements to study the effect of dilute silica gel on the critical behavior of two binary mixtures: lutidine-water and isobutyric acid–water. We have made systematic studies of mixtures of various concentrations spanning the critical region, imbibed in gels of a variety of crossover lengths. We have focused on equilibrium behavior in what would be the one-phase region of the pure system.

Measurements of the total scattered intensity reveal that the preferential attraction of one species of the mixture leads to time-independent concentration fluctuations of the fluid mixture. This is the static response of the system to the field imposed by the gel and plays a dominant role in the behavior of the gel-mixture samples in the one-phase region. We have measured the temperature and q dependence of this response and have found that the response increases strongly as the two-phase boundary of the pure system is approached. Analysis of our scattering results in terms of a simple model involving two regions, one consisting of silica and adsorbed fluid, and the other consisting of the remaining mixture, allowed us to estimate the concentration of the remaining mixture. These estimates revealed a strong shift in the concentration of the nonadsorbed fluid toward the side of the phase diagram poor in the preferentially attracted species as the two-phase boundary of the pure system was approached, and indicated that considerable care would be required to ensure that the free fluid reach the critical temperature at the critical concentration. Since the adsorbed fluid (as we have defined it) exhibits no critical fluctuations, this might be a necessary condition for reaching the critical region of the gel-mixture system.

Scattering from LW-gel samples revealed no time-dependence; however, measurements of the time dependence of the scattered light in IBAW-gels revealed three dynamic regimes. Far from the coexistence curve, where the correlation length was much smaller than the crossover length of the gel, the relaxation of concentration fluctuations was exponential, as would be observed in the pure system. Closer to the coexistence curve, the relaxation became nonexponential, and a correlation function involving either a stretched exponential or an activated form could be fit to the data. In both of these regimes, the decay was diffusive and the diffusion coefficient could be measured. The diffusion coefficient was found to be generally smaller than that of the pure system at the same temperature and average concentration as the mixture in the gel, but comparable to that of a mixture at the concentration estimated for the non-adsorbed fluid. At temperatures where the correlation length became comparable to the crossover length of the gel, an extra slow component suddenly appeared in the correlation function. The onset of slow dynamics was accompanied by overshoots and hysteresis in the static intensity. We associate this regime with the onset of phase-separation in the gel-mixture system. Indeed, samples left in the two-phase region for months eventually cleared, revealing that long-range order can occur in these systems.

ACKNOWLEDGMENTS

This research was supported by the National Science Foundation Grant Nos. DMR 90-18089 and DMR 93-20726 and by NSERC. The authors gratefully acknowledge helpful conversations with Professor Andrea Liu and Dr. Arthur Bailey.

[1] L. Monette, A.J. Liu, and G.S. Grest, Phys. Rev. A **46**, 7664 (1992).
[2] D.S. Fisher, G.M. Grinstein, and A. Khurana, Phys. Today **41** (12), 56 (1988), and references therein.
[3] Y. Imry and S.-K. Ma, Phys. Rev. Lett. **35**, 1399 (1975).
[4] S. Fishman and A. Aharony, J. Phys. C **12**, 1729 (1979).
[5] V. Jaccarino and A.R. King, Physica A **163**, 291 (1990), and references therein.
[6] D.P. Belanger, in *Recent Progress in Random Magnets,* edited by D.H. Ryan (World Scientific Publishing Co., Singapore, 1992).
[7] F. Brochard and P.G. de Gennes, J. Phys. Lett. **44**, L785 (1983).
[8] P.G. de Gennes, J. Phys. Chem. **88**, 6469 (1984).
[9] D.A. Huse, Phys. Rev. A **36**, 5383 (1987).
[10] B.J. Frisken and D.S. Cannell, Phys. Rev. Lett. **69**, 632

(1992).
[11] S.B. Dierker and P. Wiltzius, Phys. Rev. Lett. **58**, 1865 (1987); P. Wiltzius, S.B. Dierker, and B.S. Dennis, Phys. Rev. Lett. **62**, 804 (1989).
[12] S.B. Dierker and P. Wiltzius, Phys. Rev. Lett. **66**, 1185 (1991).
[13] M.Y. Lin, S.K. Sinha, J.M. Drake, X.-L. Wu, P. Thiyagarajan, and H.B. Stanley, Phys. Rev. Lett. **72**, 2207 (1994).
[14] A.J. Liu, D.J. Durian, E. Herbolzheimer, and S.A. Safran, Phys. Rev. Lett. **65**, 1897 (1990); A.J. Liu and G.S. Grest, Phys. Rev. A **44**, R7894 (1991).
[15] J.V. Maher, W.I. Goldburg, D.W. Pohl, and M. Lanz, Phys. Rev. Lett. **53**, 60 (1984); K.-Q. Xia and J.V. Maher, Phys. Rev. A **36**, 2432 (1987).
[16] W.I. Goldburg, in *Scaling Phenomena in Disordered Systems*, edited by R. Pynn and A. Skjeltorp (Plenum, New York, 1985), p. 151.
[17] K.-Q. Xia and J.V. Maher, Phys. Rev. A **37**, 3626 (1988).
[18] A.P.Y. Wong and M.H.W. Chan, Phys. Rev. Lett. **65**, 2567 (1990).
[19] A.P.Y. Wong, S.B. Kim, J. Ma, W.I. Goldburg, and M.H.W. Chan, Phys. Rev. Lett. **70**, 954 (1993).
[20] A. Maritan, M.R. Swift, M. Cieplak, M.H.W. Chan, M.W. Cole, and J.R. Banavar, Phys. Rev. Lett. **67**, 1821 (1991).
[21] F. Aliev, W.I. Goldburg, and X-L. Wu, Phys. Rev. E **47**, R3834 (1993).
[22] S. Dietrich, in *Phase Transitions and Critical Phenomena,* edited by C. Domb and J.L Lebowitz (Academic Press, San Diego, 1988), Vol. 12.
[23] M.E. Fisher and P.G. de Gennes, C.R. Acad. Sci. Ser. B **287**, 207 (1978).
[24] F. Ferri, B.J. Frisken, and D.S. Cannell, Phys. Rev. Lett. **67**, 3626 (1991).
[25] B.J. Frisken, F. Ferri, and D.S. Cannell, Phys. Rev. Lett. **66**, 2754 (1991).
[26] D. Avnir and V.R. Kaufman, J. Non-Cryst. Solids **92**, 180 (1987); B. Cabane, M. Dubois, F. Lefaucheux, and M.C. Robert, *ibid.* **119**, 121 (1990).
[27] H.R. Haller, C. Destor, and D.S. Cannell, Rev. Sci. Instrum. **54**, 973 (1983).
[28] S.K. Sinha, T. Freltoft, and J. Kjems, in *Kinetics of Aggregation and Gelation*, edited by F. Family and D.P. Landau (North-Holland, Amsterdam, 1984), p. 87; T. Freltoft, J.K. Kjems, and S.K. Sinha, Phys. Rev. B **33**, 269 (1986).
[29] B.J. Frisken, D.S. Cannell, M.Y. Lin, and S.K. Sinha, this issue, Phys. Rev. E **51**, 5866 (1995).
[30] G. Dietler, C. Aubert, and D.S. Cannell, Phys. Rev. Lett. **57**, 3117 (1986).
[31] J.G. Shanks and J.V. Sengers, Phys. Rev. A **38**, 885 (1988). We omitted the factor of $\sin\theta$ in Eq. [2.12], which we believe to be in error.
[32] B.J. Frisken, F. Ferri, and D.S. Cannell, in *Dynamics in Small Confining Systems*, edited by J.M. Drake, J. Klafter, R. Kopelman, and D.D. Awschalom, MRS Symposia Proceedings No. 290 (Materials Research Society, Pittsburgh, 1992), p. 59.
[33] H.C. Burstyn and J.V. Sengers, Phys. Rev. A **25**, 448 (1982).
[34] H. Guttinger and D.S. Cannell, Phys. Rev. A **22**, 285 (1980).
[35] H.C. Burstyn, J.V. Sengers, and P. Esfandiari, Phys. Rev. A **22**, 282 (1980).
[36] J.D. Cox and E.F.G. Herington, Trans. Faraday Soc. **52**, 926 (1956).
[37] D. Woermann and W. Sarholz, Ber. Bunsenges. Phys. Chem. **69**, 319 (1965).
[38] P.N. Pusey and W. van Megen, Physica **157A**, 705 (1989).
[39] Although the second term of Eq. (29) diverges as $\tau \to 0$, in practice the parameter τ_0 remained comparable to the smallest τ measured, and thus the $\tau \to 0$ limit of this term was A_2 for all practical purposes.
[40] See, for example, G. Williams, J. Non-Cryst. Solids **131**, 1 (1991).
[41] A.T. Ogielski and D.A. Huse, Phys. Rev. Lett. **56**, 1298 (1986).